Patients and tissue samples

The formalin-fixed, paraffin-embedded tissue sections of 59 cases of normal endometrium and 118 cases of endometrial cancer were obtained from 177 patients who underwent surgical resections at Osaka University Hospital, Japan, between 1998 and 2007. Cases of normal endometrium were obtained from 59 patients who underwent simple hysterectomy for benign indications such as leiomyoma and uterine prolapse. Histological features of the tissues were reviewed by board-certified pathologists. The degree of histological differentiation and surgical pathological staging of 118 cases of endometrial cancer were assigned according to the 1988 recommendations of International Federation of Gynecology and Obstetrics. A summary of clinicopathological information for these patients is shown in Supporting Information Table S1. Written informed consent was obtained for all the cases and the experimental protocol was approved by the ethics committees of Osaka University and National Institute of Biomedical Innovation.

Immunohistochemistry

Sections were prepared from formalin-fixed, paraffin-embedded tissue specimens, deparaffinized, and rehydrated in graded alcohols. Immunohistochemical staining for BST2 was performed using the avidin-biotin-peroxidase complex (ABC) method using a rabbit polyclonal anti-BST2 antibody (Sigma-Aldrich, St. Louis, MO) and the Vectastain ABC kit (Vector Laboratories, Burlingame, CA) according to the manufacturer's protocol. Immunostained sections were photographed with an Olympus FSX100 (Olympus, Tokyo, Japan). Detailed information is provided in the Supporting Information Materials and Methods section.

Evaluation of immunohistostaining

Immunostainings were scored according to the intensity of the staining (no staining = 0, weak staining = 1, moderate staining = 2, strong staining = 3) and the extent of stained cells (0–9% = 0, 10–40% = 1, 41–70% = 2, 71–100% = 3). The final immunohistochemistry (IHC) score was determined by multiplying the intensity score (0, 1, 2, or 3) with the positivity score (0, 1, 2, or 3), resulting in a maximum score of 9. Three independent gynecologic oncologists (Y.U., K.Y., and M.F.), blinded to the histological data, analyzed the stained sections using an Olympus BH2 microscope (Olympus). In case of disagreement, the staining results were re-evaluated by careful discussion until a consensus was reached.

Cell proliferation assay

Endometrial cancer cells plated in 96-well plates (1,000 cells per well) were grown in their respective media for 24, 48, or 72 hr after the addition of antibody or small interfering RNA (siRNA) transfection. At each time point, cell proliferation was assessed by a WST-8 assay according to the manufacturer's protocol (Nacalai Tesque). Detailed information for these assays can be found in the Supporting Information Materials and Methods section.

ADCC assay

ADCC was measured by calcein-acetoxymethyl ester (calcein-AM) release assay, with sensitivity similar to the traditional ^{51}Cr release assay.[16,17] Detailed information for this assay can be found in the Supporting Information Materials and Methods section.

CDC assay

CDC was evaluated using a ^{51}Cr release assay.[18] Detailed information for this assay can be found in the Supporting Information and Methods section.

Tumor xenograft and antibody therapy

Healthy female severe combined immunodeficient (SCID) and nonobese diabetic (NOD)/SCID mice at 8 weeks of age were obtained from Charles River Japan (Yokohama, Japan) and maintained in a specific pathogen-free facility. For subcutaneous xenograft experiments, SCID mice were inoculated subcutaneously with 5×10^6 HEC-88nu or SNG-II cells in a total volume of 50 μl of 1/1 (v/v) PBS/Matrigel (Becton Dickinson) into the abdomen. NOD/SCID mice were inoculated with 5×10^6 HEC-88nu cells. PBS, isotype control (mouse IgG2aκ, Sigma-Aldrich), or mouse anti-human BST2 antibody (clone 1B4: Chugai Pharmaceutical) was administered intraperitoneally at a dose of 5 mg/kg (SNG-II) or 10 mg/kg (HEC-88nu) in 400 μl of PBS. Six mice were used per group. The first dose was given on day 4 (SNG-II) or 9 (HEC-88nu) and continued twice weekly for 4 weeks. Tumors were measured twice weekly from days 4 (SNG-II) or 9 (HEC-88nu) using vernier calipers throughout the study. Tumor volumes were calculated using the following formula: tumor volume (mm^3) = length × width × height. After 8 (HEC-88nu) or 12 (SNG-II) weeks, tumors were resected and weighted. All animal experiments were conducted according to the institutional ethical guidelines for animal experimentation of the National Institute of Biomedical Innovation.

Statistical analysis

For immunohistochemistry, statistical significance of difference between normal endometrium and endometrial cancer was analyzed by the nonparametric Mann–Whitney *U* test. Differences in the *in vitro* cytotoxic assay were determined by using the Kruskal–Wallis test followed by the Steel procedure. For all subcutaneous tumor comparisons, groups were analyzed using the Kruskal–Wallis test followed by the Steel-Dwass procedure.

Results

Protein expression profiles in normal endometrium and endometrial cancer

To identify potential therapeutic targets of endometrial cancer, we performed comparative protein expression profiling between normal endometrium (EM-E6/E7/TERT cells) and

endometrial cancer (HEC-1, HEC-1A, HEC-6, HEC-108, HEC-116, HEC-251, and SNG-II cells) at the cell surface level. We identified a total of 272 proteins by a biotinylation-based approach for cell membrane enrichment combined with iTRAQ technology using nano LC-MS/MS analysis. The complete list of all the proteins identified is shown in Supporting Information Table S2. The list of proteins identified with single peptide is provided in Supporting Information Table S3. MS/MS spectra of all single-peptide-based assignments with masses detected as well as fragment assignments are presented in Supporting Information Table S4. The raw MS data of this analysis is publicly available for download from PeptideAtlas (available at: http://www.peptideatlas.org/PASS/PASS00032). To correct the error of quantitation during chromatographic procedures, we added the equivalent moles of the sulfo-NHS-SS-biotin labeled BSA into the each sample as an internal standard. The iTRAQ ratio of BSA (0.873 to 1.131, Supporting Information Table S3) was used for the correction of quantitation information accurately. According to the annotation from UniprotKB and Ingenuity Pathway Analysis, 139 proteins (51% of the identified proteins) were located in the plasma membrane (Fig. 1*a*). Among these 139 plasma membrane proteins identified, 11 proteins were increased more than twofold in at least four of seven endometrial cancer cell lines compared with the normal endometrial cell line (Table 1). As expected, neural cell adhesion molecule L1, a plasma membrane protein previously known to be overexpressed in endometrial cancer, was identified again. Interestingly, BST2 was found to show one of the most significant differences in expression between normal endometrial cells and endometrial cancer cells, making it a prime target.

Confirmatory studies by qRT-PCR and FACS

To confirm the altered expression of BST2 in endometrial cancer, we first evaluated its transcripts by qRT-PCR in the normal endometrial cell line (EM-E6/E7/TERT cells) and nine endometrial cancer cell lines (HEC-1, HEC-1A, HEC-6, HEC-88nu, HEC-108, HEC-116, HEC-251, SNG-II, and SNG-M cells). BST2 mRNA expression was clearly detected in seven of the nine endometrial cancer cell lines, while the normal endometrial cell line showed no detectable expression of BST2 transcripts (Fig. 1*b*).

We then evaluated the expression of BST2 at the protein level and confirmed the surface localization of BST2 by FACS analysis. Protein expression of BST2 was very weak in EM-E6/E7/TERT cells. In contrast, a considerably higher level of BST2 protein expression was detected in six of the nine endometrial cancer cell lines on the cell surface (Fig. 1*c*). Together our data demonstrate that BST2 was overexpressed in endometrial cancer cells at both the mRNA and protein level; this was consistent with our iTRAQ analysis.

Validation study by IHC

As a validation study, immunohistochemical analyses were performed by examination of the BST2 expression pattern in paraffin-embedded tissue samples (Supporting Information Table S1). Representative immunohistochemical staining of BST2 in tissue sections from patients revealed intense BST2 staining in endometrial cancer compared with normal endometrium (Fig. 2*a*). In addition, immunohistochemical analyses showed membranous immunoreactivity in endometrial cancer cells, indicating that the localization of BST2 was at cell surface. We observed significantly stronger positive staining of BST2 in tissue sections from patients with endometrial cancer compared with normal endometrium ($p < 0.0001$) (Fig. 2*b*). In 118 endometrial cancer specimens, moderately to strongly positive staining (IHC score = 3–9) was detected in 71.2% of specimens (84 of 118), whereas only 1.7% (1 of 59) were positive in the normal endometrial specimens. There were no significant differences in BST2 immunohistochemical staining among endometrial cancer tissues according to their degree of histological differentiation or surgical pathological staging ($p = 0.77$ and 0.06, respectively, by the Kruskal–Wallis test). There were no significant differences in BST2 staining among normal proliferative-phase, secretory-phase, and atrophic endometrium ($p = 0.82$ by the Kruskal–Wallis test). These results indicate that BST2 was overexpressed on the cell surface of endometrial cancer tissues much more frequently than in normal endometrium, raising the possibility that BST2 might represent a potential therapeutic target.

BST2-siRNA and anti-BST2 antibody treatment *in vitro*

To examine whether the BST2 expression contributes to cell proliferation of endometrial cancer cells, the effect of BST2-siRNA treatment in four of the endometrial cancer cell lines expressing BST2 (HEC-6, HEC-88nu, HEC-116, and SNG-II cells) was evaluated using the WST-8 assay. To ensure silencing efficiency, BST2 expression was analyzed by FACS analysis after 48 hr of siRNA transfection. The two siRNAs targeting BST2 (Hs_BST2_1 and Hs_BST2_5) had a similar silencing effect on the protein level (Supporting Information Fig. S1). There were no significant differences in cell proliferation among BST2-siRNA and control-siRNA treated cells (Fig. 3*a*). Similarly, anti-BST2 antibody treatment did not affect *in vitro* cell proliferation (Fig. 3*b*).

We subsequently examined whether an anti-BST2 antibody can induce ADCC among endometrial cancer cells using the calcein-AM release assay. To study the specificity of anti-BST2 antibody-mediated ADCC against BST2-expressing target cells, an ADCC assay was performed using a BST2-expressing endometrial cancer cell line (HEC-88nu cells) and a BST2-negative cell line (HEC-1 cells). As shown in Figure 3*c*, HEC-88nu cells treated with the anti-BST2 antibody showed specific lysis *via* ADCC ($p = 0.045$), whereas the anti-BST2 antibody showed no lytic activity against HEC-1 cells.

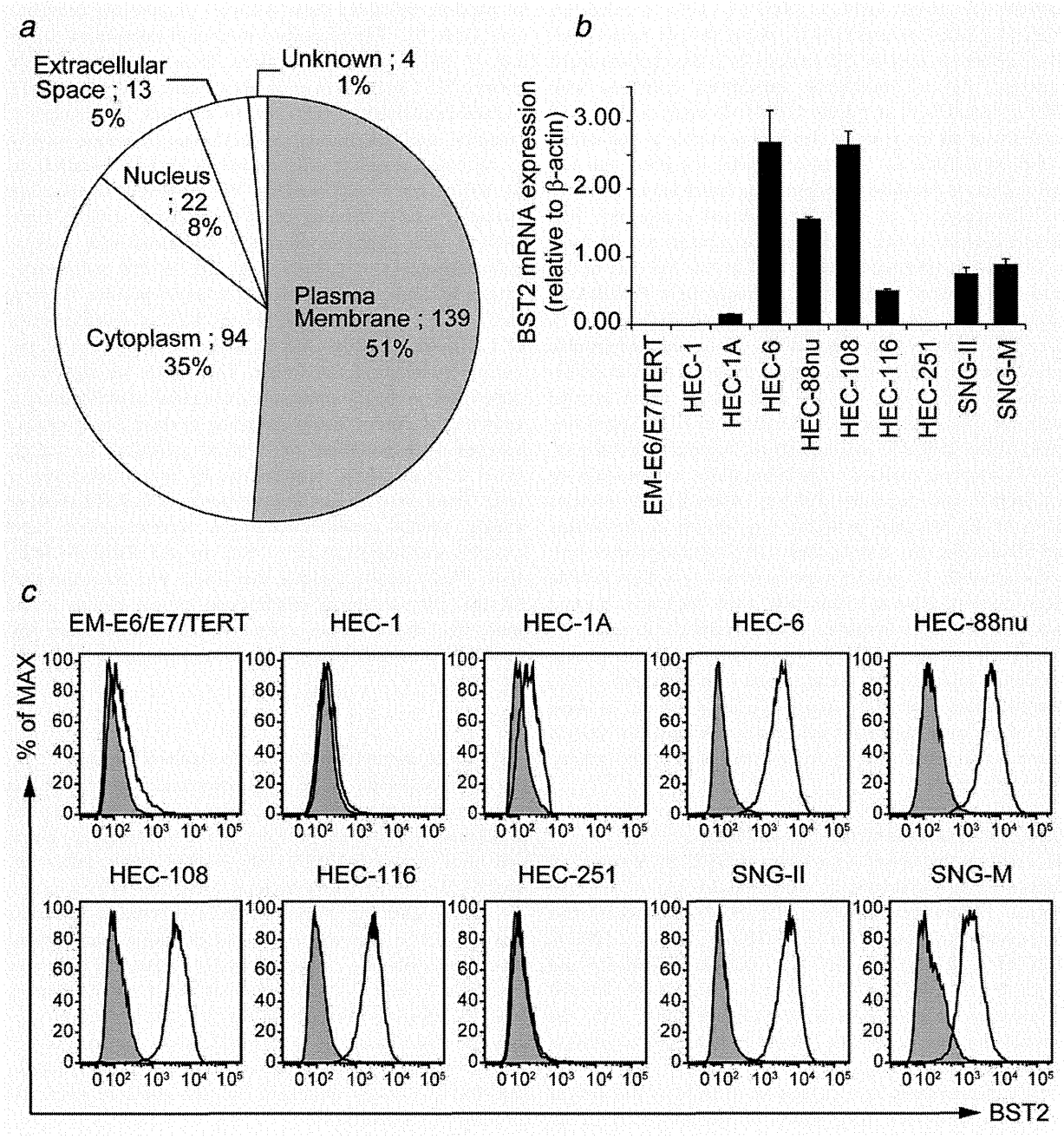

Figure 1. (*a*) Subcellular localization of the identified 272 proteins analyzed by UniprotKB and Ingenuity Pathway Analysis. (*b*) Confirmation of iTRAQ results by qRT-PCR. qRT-PCR was used to quantify BST2 mRNA; β-actin was used as the internal control. Data are mean ± SEM of three independent experiments, each performed in triplicate. BST2 mRNA expression was not detected in the normal endometrial cell line (EM-E6/E7/TERT cells), but seven of nine endometrial cancer cell lines exhibited positive expression of BST2 mRNA. (*c*) Confirmation of iTRAQ results by FACS analysis. The shaded histogram profile indicates the isotype control, and the open histogram indicates the anti-BST2 antibody staining results.

We also examined CDC exhibited by the anti-BST2 antibody. Figure 3*d* shows that the BST2-expressing endometrial cancer cell line (HEC-88nu cells), but not the BST2-negative cell line (HEC-1 cells), was sensitive to CDC ($p = 0.045$).

Therapeutic effect of the anti-BST2 antibody *in vivo*

To evaluate the therapeutic efficacy of anti-BST2 antibody therapy, *in vivo* studies were performed using an endometrial cancer xenograft model. SCID mice injected with either

Table 1. Plasma membrane proteins overexpressed in endometrial cancer cells

Accession number	Protein name	No. peptides used for identification	iTRAQ ratio						
			HEC-1	HEC-1A	HEC-6	HEC-108	HEC-116	HEC-251	SNG-II
O14672	Disintegrin and metalloproteinase domain-containing protein 10	5	1.670	1.271	2.032	3.175	2.824	3.958	1.364
P11279	Lysosome-associated membrane glycoprotein 1	1	0.398	3.017	5.745	8.722	4.307	5.239	1.727
P25942	Tumor necrosis factor receptor superfamily member 5	2	2.518	5.353	7.796	6.438	8.526	2.747	n.d.
P31431	Syndecan-4	5	n.d.	n.d.	0.949	11.644	2.905	4.396	8.121
P32004	Neural cell adhesion molecule L1	26	1.211	0.905	2.171	9.025	2.603	13.756	4.283
P50895	Basal cell adhesion molecule	15	0.692	0.876	5.378	2.493	2.363	3.936	2.864
P78310	Coxsackievirus and adenovirus receptor	3	1.773	3.140	5.228	16.042	4.507	3.265	3.256
Q10589	Bone marrow stromal antigen 2	2	n.d.	6.438	85.276	94.318	87.278	3.435	38.946
Q14126	Desmoglein-2	9	2.360	3.199	1.912	2.827	5.286	2.542	4.637
Q9H5V8	CUB domain-containing protein 1	2	0.907	2.234	11.680	3.508	11.603	8.623	17.020
Q9Y624	Junctional adhesion molecule A	1	4.374	17.088	25.645	47.784	23.673	77.025	18.523

The iTRAQ ratios were calculated comparing the endometrial cancer cells' iTRAQ signal divided by the normal endometrial cells' iTRAQ signal. Proteins overexpressed more than twofold in at least four cell lines are listed.
Abbreviations: n.d. = Not detected.

HEC-88nu or SNG-II cells (BST2-expressing endometrial cancer cell lines) were assigned to one of three treatment groups ($n = 6$ per group): (*i*) PBS; (*ii*) isotype control; (*iii*) anti-BST2 antibody, 5 mg/kg (SNG-II) or 10 mg/kg (HEC-88nu) twice weekly. Although the tumors of all mice were approximately equal in initial volumes, significant differences in tumor growth were observed during the study, as illustrated by the tumor growth curve in Figure 4*a*. All mice were sacrificed on days 61 (HEC-88nu) or 85 (SNG-II) post-tumor inoculation. The tumors of the anti-BST2 antibody treatment group were markedly smaller than that of the PBS and control IgG treatment groups (Fig. 4*b*). The tumor weights of the anti-BST2 antibody treatment group were significantly decreased compared with the PBS and control IgG treatment groups, whereas there was no statistical difference between the PBS and control IgG treatment groups at the termination of the experiment (Fig. 4*c*).

Once we had established a proof of principle that the anti-BST2 antibody can inhibit tumor growth, we then sought to identify mechanisms by which the anti-BST2 antibody acts on tumor cells. Anti-BST2 antibody treatment showed no significant therapeutic effect in identically treated NOD/SCID mice, with anti-BST2 antibody treated mice developing tumors at virtually the same rate as PBS and control IgG treated mice (Fig. 5).

Discussion

Our study focused on a novel biotechnological method we found to be useful for identifying tumor-associated cell-surface antigens differentially expressed in cancer cells with respect to corresponding normal cells. The ideal expression pattern of a tumor-specific antigen for antibody therapy is that it should be abundant and homogeneous on the surface of cancer cells, and absent from normal tissue.[19] Such targets can be experimentally identified at different molecular levels, such as DNA, RNA, and protein.

DNA microarray technologies have led to the identification of genes that are dysregulated in cancer cells when compared with normal cells.[20,21] However, DNA arrays measure only the changes at the mRNA level, and this is not always translated to corresponding changes at the protein level, leading to many false positives and missed positives. The use of mRNA expression patterns by themselves is often insufficient for understanding the expression of protein products, as additional post-translational mechanisms, including protein translation, post-translational modification, and degradation, may influence the level of a protein and its antigenic epitopes.[22,23] In addition, effective induction of ADCC or CDC mediated by a therapeutic antibody requires abundant expression of cell-surface proteins specifically on the cancer cells,[24,25] providing a compelling rationale for a more direct analysis of gene expression at the protein level by proteomic methods.

The intensity of individual proteins in the sample is crucial when performing proteomic analyses, as larger amounts

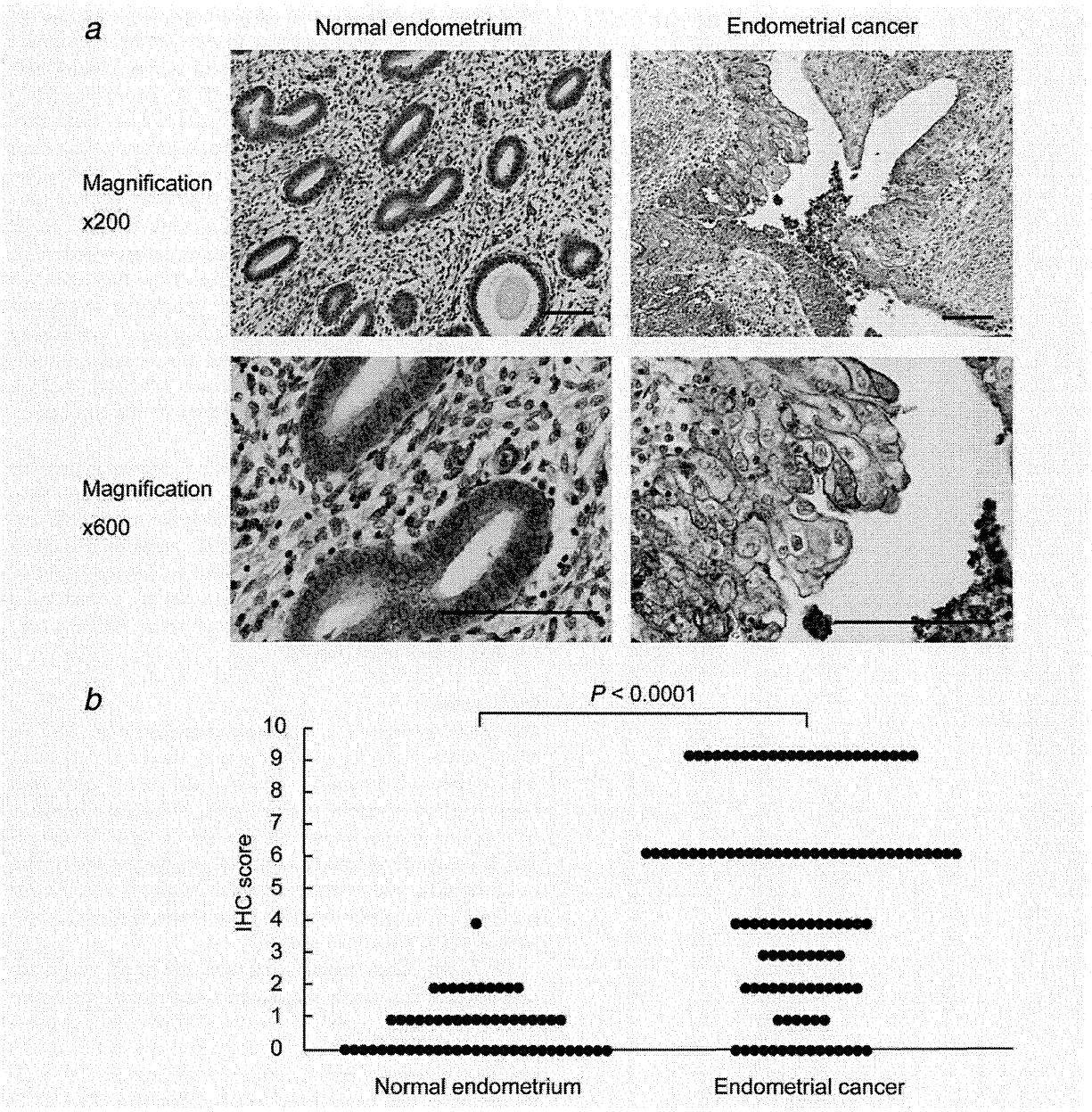

Figure 2. (*a*) Representative immunohistochemical staining for BST2 in normal endometrium and endometrial cancer specimens. Immunostained sections were counterstained with hematoxylin and photographed with an Olympus FSX100 (Olympus). The expression of BST2 was negative in normal endometrium, whereas endometrial cancer showed strong membranous reactivity for BST2. Scale bar, 100 μm. (*b*) BST2 immunoreactivity in normal endometrial tissues and endometrial cancer tissues. The expression of BST2 was increased in endometrial cancer, with significant difference ($p < 0.0001$). IHC score = intensity score (0, 1, 2, or 3) × positivity score (0, 1, 2, or 3).

of some proteins may hinder the detection of less abundant proteins, such as cell-surface membrane proteins. As such, enrichment of plasma membrane proteins is an important initial step. Physical isolation of membrane proteins using centrifugation and/or chemical extraction are well-described methods.[26,27] However, these techniques fail to isolate only the cell-surface membrane proteins and usually provide extracts that consist of all the membrane structures, including those inside the cell (e.g., endoplasmic reticulum, Golgi apparatus, and mitochondrial membranes). The proteins that are found inside the cell will most likely not be accessible to the systemically delivered antibodies and hence do not represent a group of interest for discovery of targetable molecules. Another way to enrich specifically the potentially accessible

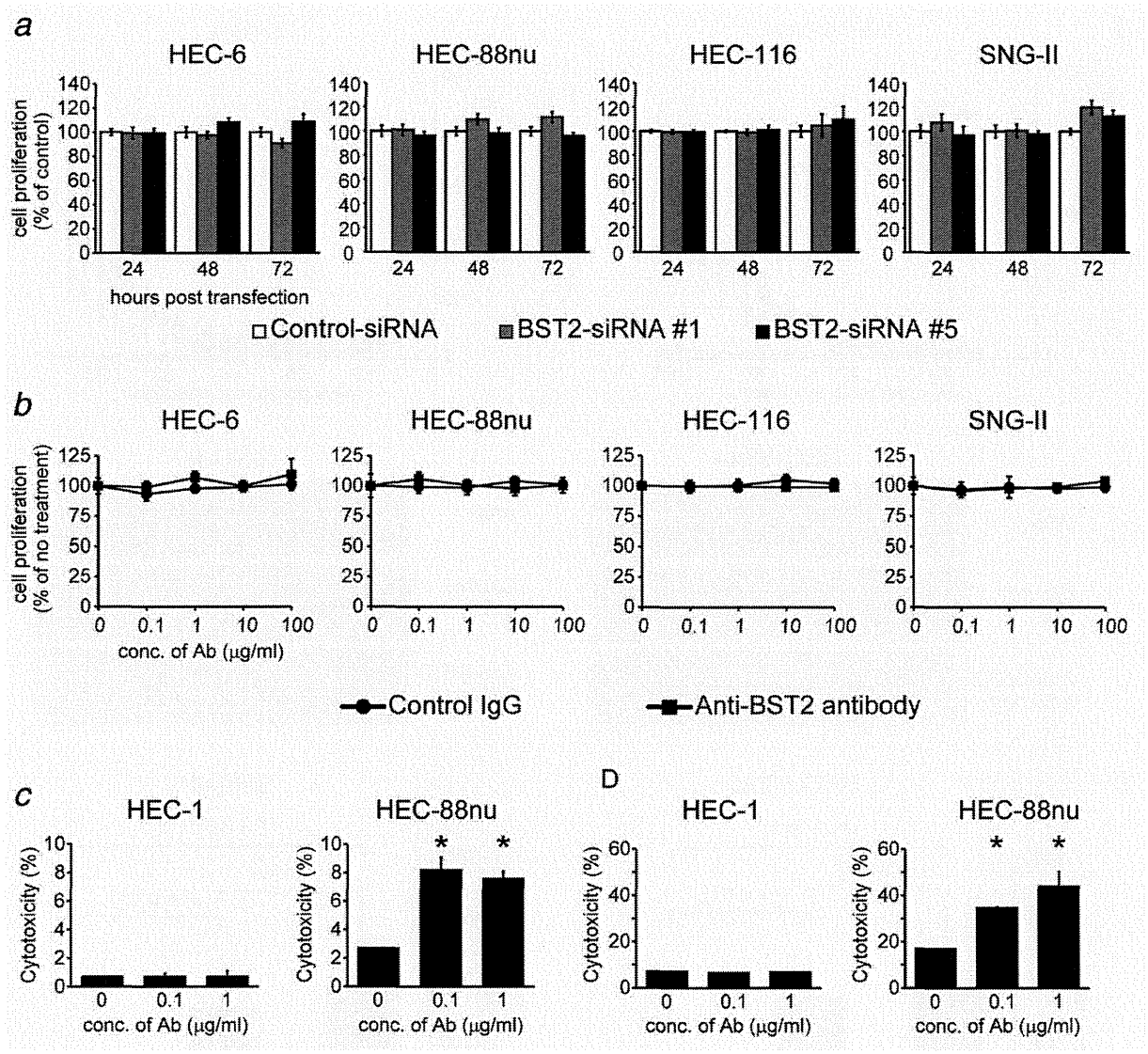

Figure 3. *In vitro* growth assay of endometrial cancer cells treated with BST2-siRNA (*a*) or anti-BST2 antibody (*b*). HEC-6, HEC-88nu, HEC-116, and SNG-II cells are BST2-positive endometrial cancer cell lines. (*a*) A total of 1,000 cells were plated in each well of 96-well plates and then siRNA was transfected. Cell proliferation was assessed at 24, 48, and 72 hr using a WST-8 assay. Values were normalized to control-siRNA treated cells. There were no significant differences in cell proliferation among BST2-siRNA and control-siRNA treated cells. (*b*) Anti-BST2 antibody or isotype-control IgG (final concentrations of 0.1, 1, 10, or 100 μg/ml) were added to 1,000 cells/well in 96-well plates. Cell proliferation was assessed at 72 hr using the WST-8 assay. Values were normalized to untreated cells. Anti-BST2 antibody had no direct cytotoxic effect on endometrial cancer cells *in vitro*. (*c*), ADCC activity of anti-BST2 antibody. Calcein-labeled HEC-1 (BST2-negative) and HEC-88nu (BST2-positive) cells were incubated with bone marrow-derived lymphokine-activated killer cells at an *E/T* ratio of 50 in the presence of 0, 0.1, or 1.0 μg/ml anti-BST2 antibody. (*d*) CDC activity of anti-BST2 antibody. ^{51}Cr-labeled HEC-1 (BST2-negative) and HEC-88nu (BST2-positive) cells were incubated with 12.5% baby rabbit complement in the presence of 0, 0.1, or 1.0 μg/ml anti-BST2 antibody. Anti-BST2 antibody had ADCC and CDC activity against HEC-88nu cells (BST2-expressing endometrial cancer cell line). *$p = 0.045$.

cell-surface proteins involves conjugating membrane proteins with the small molecule biotin and using the receptor streptavidin to extract the labeled proteins.[28,29]

In this study, we quantitatively analyzed the plasma membrane profiles comparing normal endometrium and endometrial cancer using a biotinylation-based approach for cell membrane enrichment combined with iTRAQ technology using nano LC-MS/MS analysis. While quantitative membrane proteomic approaches combining biotin labeling followed by enrichment of cell surface membrane proteins by avidin-beads and SILAC technology or spectral counting were already reported,[28,30] we demonstrated that iTRAQ approach is also an alternative method, suitable for the quantitative analysis of the cell surface membrane proteins.

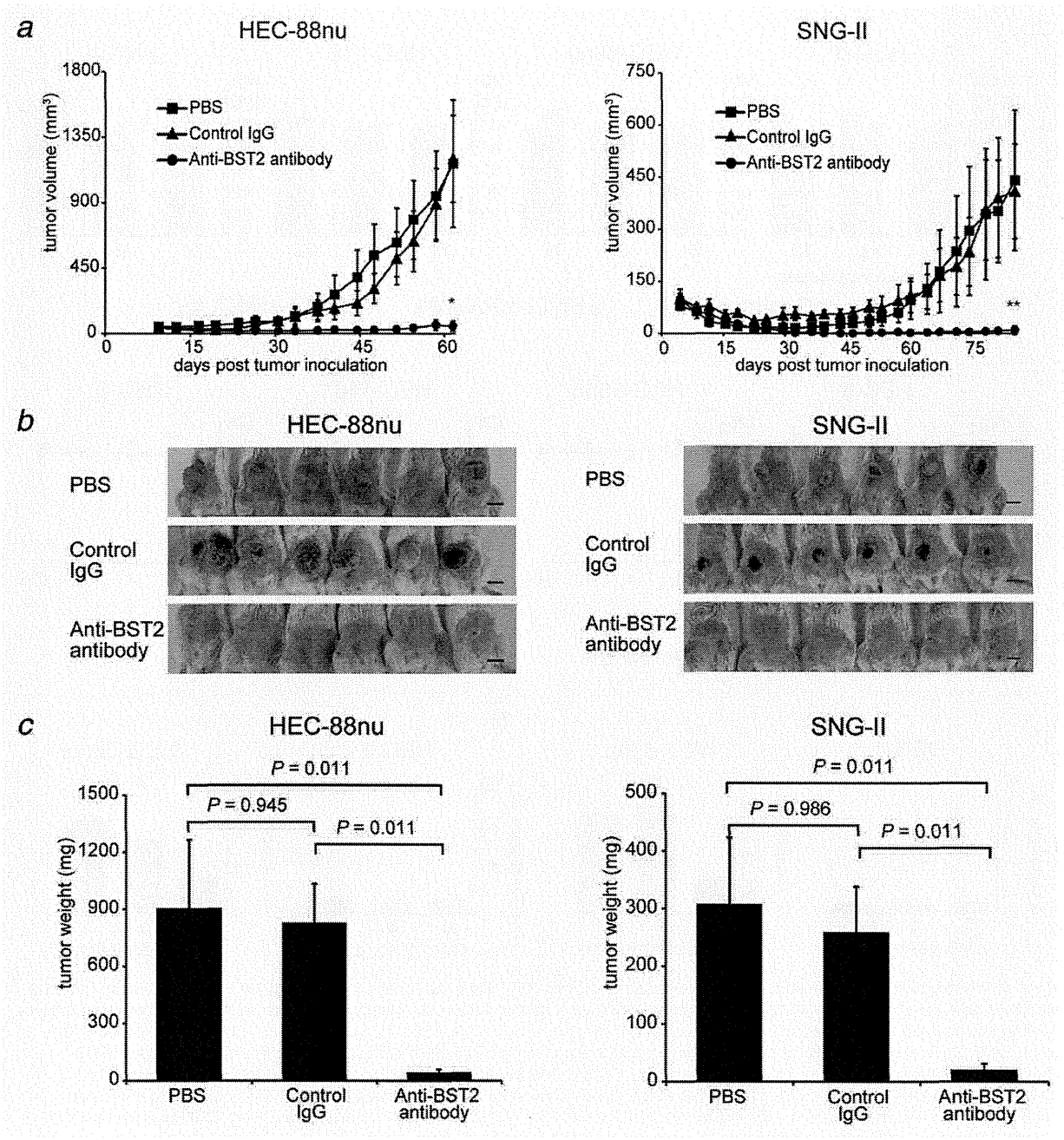

Figure 4. *In vivo* therapeutic effect of anti-BST2 antibody on endometrial cancer growth. SCID mice inoculated with HEC-88nu or SNG-II cells (both are BST2-expressing endometrial cancer cell lines) received PBS, control IgG, or anti-BST2 antibody twice a week for 4 weeks from days 4 (SNG-II) or 9 (HEC-88nu) post-tumor inoculation. (*a*) Time-course of tumor volume change. Tumor volumes were measured twice a week and calculated as the product of length, width, and height. The mean volume ± SD of six tumors in each group is shown. Anti-BST2 antibody treatment resulted in significantly decreased tumor growth compared with the other control groups (PBS and control IgG) at the termination of the experiment. $*p = 0.0110$, $**p = 0.0108$. (*b*) Mice at the end of the experiment. Scale bar, 1 cm. (*c*) Tumor weight at autopsy. After 4 (HEC-88nu) or 8 (SNG-II) weeks of observation following treatment, tumors were removed and weighted. Their weights were significantly different between the experimental (anti-BST2 antibody) group and the control (PBS and control IgG) groups ($p = 0.011$).

In total, we identified 272 proteins, 139 of which (51%) were found to be cell-surface proteins. Given that global genomic analysis predicts that 20 to 30% of all open reading frames encode integral membrane proteins,[31] our results indicate that the membrane proteins were moderately enriched by our sample preparation strategy.

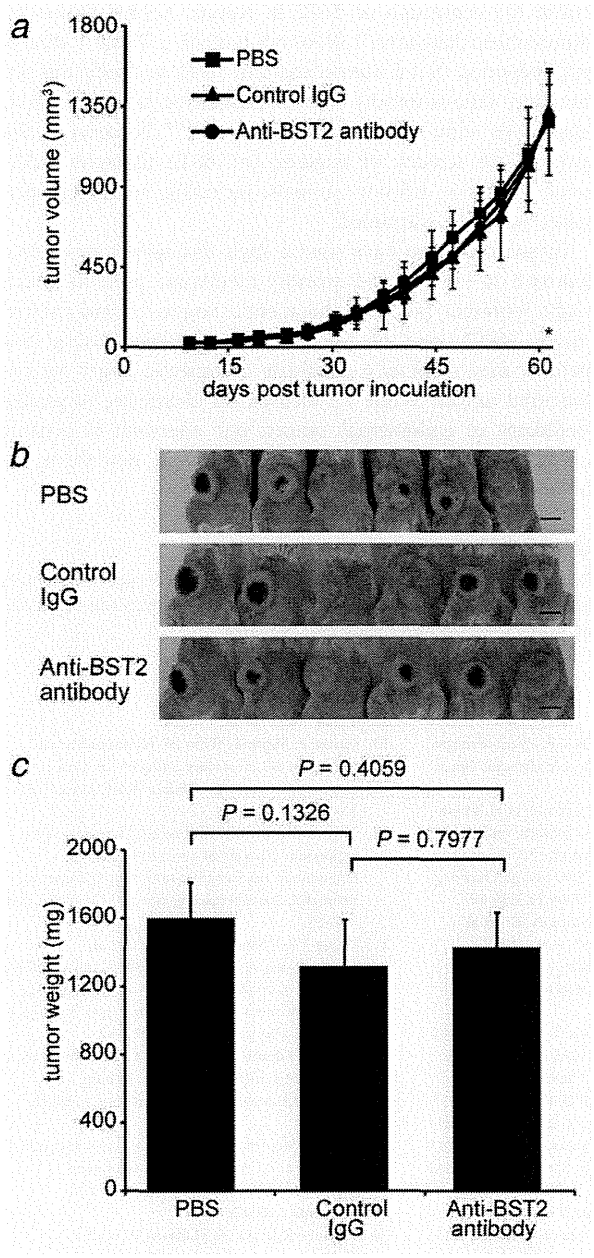

Figure 5. Natural killer cells are required for antitumor activity of anti-BST2 antibody *in vivo*. NOD/SCID mice inoculated with HEC-88nu cells (BST2-expressing endometrial cancer cell line) received PBS, control IgG, or anti-BST2 antibody twice a week for 4 weeks from day 9 post-tumor inoculation. (*a*) Time-course of tumor volume change. Tumor volumes were measured twice a week and calculated as the product of length, width, and height. The mean volume ± SD of six tumors in each group is shown. There were no significant differences in tumor volumes among PBS, control IgG, and anti-BST2 antibody groups at the termination of the experiment. $*p = 0.9769$. (*b*) Mice at the end of the experiment. Scale bar, 1 cm. (*c*) Tumor weight at autopsy. After 4 weeks of observation following treatment, tumors were removed and weighted. There were no significant differences in tumor weights among the three groups.

Eleven proteins were annotated as unique membrane proteins whose expression was specifically up-regulated in endometrial cancer (Table 1). These proteins included several reported markers for prediction of clinical outcome (neural cell adhesion molecule L1 and CUB domain-containing protein 1), suggesting a certain amount of robustness for our methodology of identifying tumor-associated antigens.[32,33] In the present study, BST2 was further validated as a potential therapeutic target for endometrial cancer, because BST2 showed one of the most significant differences between normal endometrium and endometrial cancer (a 10-fold up-regulation was shown in four of seven endometrial cancer cell lines compared with the normal endometrial cell line) and has been reported to be overexpressed in endometrial cancer using genome-wide gene expression profiling.[21] In future work, we would like to characterize other novel candidates for developing new therapeutic agents.

BST2 (also termed CD317, tetherin, or HM1.24) was originally identified as a Type II membrane glycoprotein with an unusual topology (one-pass transmembrane domain and C-terminal glycosylphosphatidylinositol anchor) that is preferentially overexpressed on multiple myeloma cells.[34,35] More recently, BST2 has also been proposed as a tumor-associated antigen expressed in some human cancer cell lines.[36–38] However, BST2 is an interferon-induced protein and inflammatory cytokines such as interleukin-6 and tumor necrosis factor-alpha might also induce its expression.[35] Furthermore, BST2 has been found to block the release of enveloped virus particles (e.g., HIV-1, Marburg virus, and Ebola virus) and may therefore be an important component of the antiviral innate immune defense.[39,40] Future research should further explore the role of BST2 in inflammatory diseases.

To our knowledge, protein expression of BST2 in endometrial cancer has not been described before. Our results are the first to show that BST2 is significantly overexpressed in endometrial cancer compared with normal endometrium. The degree of histological differentiation and surgical pathological staging showed no significant correlation with expression of BST2. Given the almost ubiquitous expression of BST2 in endometrial cancer, BST2 might have some value acting as a potential molecular therapeutic target.[19] In this study, we demonstrated that the administration of the anti-BST2 antibody reduced the growth of BST2-positive endometrial cancer cells in SCID mice. The suppressive effects on tumor growth were observed in two cell lines. In principle, the putative mechanisms of monoclonal antibody-based cancer therapy can be classified into two categories.[41,42] One mechanism is direct action to block the function of target signaling molecules or receptors, or stimulate apoptosis. It has been reported that BST2 gene is one of the important activators of the NF-κB pathway,[43] suggesting that the signaling from BST2 antigen affects the biological responses of BST2-expressing cells. However, silencing of BST2 expression by siRNA transfection did not alter its cell proliferation, and the anti-BST2 antibody had no direct cytotoxic effect on

BST2-positive endometrial cancer cells *in vitro*. The other mechanism of tumor growth suppression is *via* an indirect action mediated by immune systems such as the ADCC and CDC. We showed that the anti-BST2 antibody had ADCC and CDC activity against BST2-expressing endometrial cancer cells. Indeed, the same clone of this monoclonal antibody used in this study has previously been shown to be effective in promoting ADCC and CDC.[37,38] To examine the relative importance of ADCC, xenograft analysis was performed using NOD/SCID mice,[44] which have impaired natural killer cells, thereby compromising their ADCC activity. Anti-BST2 antibody treatment did not result in a significant decrease in tumor growth, suggesting that host effector mechanisms, and ADCC in particular, critically contribute to the antitumor activity of the anti-BST2 antibody *in vivo*.[45]

Beyond tumors, expression of BST2 on normal tissue is a key factor in assessing the suitability of an antigen for antibody targeting in oncology. Expression of BST2 in normal tissues is still less clear. An earlier report indicated that BST2 expression was barely detectable on normal B cells and was not detected on other normal tissues, including bone marrow, liver, heart, kidney, and spleen.[34] A recent article demonstrated the expression of BST2 in various normal tissues by immunohistochemistry.[46] Although limited, a Phase I clinical study reported that a humanized anti-BST2 antibody did not cause any serious toxicity when administered to patients with relapsed or refractory multiple myeloma.[47,48] To consider the potential for toxicity of targeted anti-BST2 therapies, additional studies in relevant animals, including nonhuman primates, would be warranted.

In summary, we have used a high-throughput proteomic approach to identify and quantify membrane proteins which might represent potential therapeutic targets of endometrial cancer. BST2, one of the proteins identified using this method, may serve as a candidate therapeutic target for endometrial cancer. While we focused on identifying targetable candidates of endometrial cancer, our approach is broadly applicable to other malignancies for screening new therapeutic targets.

Acknowledgements

The authors are grateful to Chugai Pharmaceutical for the gift of antibodies against BST2; Ms. A. Katsuhara and Ms. M. Urase for experimental assistance; Ms. Y. Kanazawa for secretarial assistance.

References

1. Marcus R, Imrie K, Belch A, et al. CVP chemotherapy plus rituximab compared with CVP as first-line treatment for advanced follicular lymphoma. *Blood* 2005;105:1417–23.
2. Slamon DJ, Leyland-Jones B, Shak S, et al. Use of chemotherapy plus a monoclonal antibody against HER2 for metastatic breast cancer that overexpresses HER2. *N Engl J Med* 2001;344: 783–92.
3. Leth-Larsen R, Lund RR, Ditzel HJ. Plasma membrane proteomics and its application in clinical cancer biomarker discovery. *Mol Cell Proteomics* 2010;9:1369–82.
4. Shin BK, Wang H, Yim AM, et al. Global profiling of the cell surface proteome of cancer cells uncovers an abundance of proteins with chaperone function. *J Biol Chem* 2003;278: 7607–16.
5. Zhao Y, Zhang W, Kho Y. Proteomic analysis of integral plasma membrane proteins. *Anal Chem* 2004;76:1817–23.
6. Ong SE, Blagoev B, Kratchmarova I, et al. Stable isotope labeling by amino acids in cell culture, SILAC, as a simple and accurate approach to expression proteomics. *Mol Cell Proteomics* 2002; 1:376–86.
7. Alex P, Gucek M, Li X. Applications of proteomics in the study of inflammatory bowel diseases: current status and future directions with available technologies. *Inflamm Bowel Dis* 2009; 15:616–29.
8. Choe L, D'Ascenzo M, Relkin NR, et al. 8-plex quantitation of changes in cerebrospinal fluid protein expression in subjects undergoing intravenous immunoglobulin treatment for Alzheimer's disease. *Proteomics* 2007;7: 3651–60.
9. Jemal A, Siegel R, Xu J, et al. Cancer statistics, 2010. *CA Cancer J Clin* 2010;60:277–300.
10. Obel JC, Friberg G, Fleming GF. Chemotherapy in endometrial cancer. *Clin Adv Hematol Oncol* 2006;4:459–68.
11. Fleming GF, Brunetto VL, Cella D, et al. Phase III trial of doxorubicin plus cisplatin with or without paclitaxel plus filgrastim in advanced endometrial carcinoma: a Gynecologic Oncology Group Study. *J Clin Oncol* 2004;22:2159–66.
12. Humber CE, Tierney JF, Symonds RP, et al. Chemotherapy for advanced, recurrent or metastatic endometrial cancer: a systematic review of Cochrane collaboration. *Ann Oncol* 2007;18:409–20.
13. Kyo S, Nakamura M, Kiyono T, et al. Successful immortalization of endometrial glandular cells with normal structural and functional characteristics. *Am J Pathol* 2003;163:2259–69.
14. Mizumoto Y, Kyo S, Ohno S, et al. Creation of tumorigenic human endometrial epithelial cells with intact chromosomes by introducing defined genetic elements. *Oncogene* 2006;25:5673–82.
15. Scheurer SB, Rybak JN, Roesli C, et al. Identification and relative quantification of membrane proteins by surface biotinylation and two-dimensional peptide mapping. *Proteomics* 2005;5:2718–28.
16. Roden MM, Lee KH, Panelli MC, et al. A novel cytolysis assay using fluorescent labeling and quantitative fluorescent scanning technology. *J Immunol Methods* 1999;226:29–41.
17. Neri S, Mariani E, Meneghetti A, et al. Calcein-acetyoxymethyl cytotoxicity assay: standardization of a method allowing additional analyses on recovered effector cells and supernatants. *Clin Diagn Lab Immunol* 2001;8:1131–5.
18. Wang W, Nishioka Y, Ozaki S, et al. Chimeric and humanized anti-HM1.24 antibodies mediate antibody-dependent cellular cytotoxicity against lung cancer cells. *Lung Cancer* 2009;63:23–31.
19. Carter P, Smith L, Ryan M. Identification and validation of cell surface antigens for antibody targeting in oncology. *Endocr Relat Cancer* 2004; 11:659–87.
20. Mutter GL, Baak JP, Fitzgerald JT, et al. Global expression changes of constitutive and hormonally regulated genes during endometrial neoplastic transformation. *Gynecol Oncol* 2001;83: 177–85.
21. Wong YF, Cheung TH, Lo KW, et al. Identification of molecular markers and signaling pathway in endometrial cancer in Hong Kong Chinese women by genome-wide gene expression profiling. *Oncogene* 2007;26:1971–82.
22. Chen G, Gharib TG, Huang CC, et al. Discordant protein and mRNA expression in lung adenocarcinomas. *Mol Cell Proteomics* 2002;1: 304–13.
23. Tian Q, Stepaniants SB, Mao M, et al. Integrated genomic and proteomic analyses of gene expression in mammalian cells. *Mol Cell Proteomics* 2004;3:960–9.
24. Mimura K, Kono K, Hanawa M, et al. Trastuzumab-mediated antibody-dependent cellular cytotoxicity against esophageal squamous cell carcinoma. *Clin Cancer Res* 2005;11: 4898–904.
25. van Meerten T, van Rijn RS, Hol S, et al. Complement-induced cell death by rituximab depends on CD20 expression level and acts complementary to antibody-dependent cellular cytotoxicity. *Clin Cancer Res* 2006;12:4027–35.
26. Patwardhan AJ, Strittmatter EF, Camp DG II, et al. Comparison of normal and breast cancer cell lines using proteome, genome, and interactome data. *J Proteome Res* 2005;4:1952–60.
27. Tan S, Tan HT, Chung MC. Membrane proteins and membrane proteomics. *Proteomics* 2008;8: 3924–32.

28. Conn EM, Madsen MA, Cravatt BF, et al. Cell surface proteomics identifies molecules functionally linked to tumor cell intravasation. *J Biol Chem* 2008;283:26518–27.
29. Kischel P, Guillonneau F, Dumont B, et al. Cell membrane proteomic analysis identifies proteins differentially expressed in osteotropic human breast cancer cells. *Neoplasia* 2008;10: 1014–20.
30. Qiu H, Wang Y. Quantitative analysis of surface plasma membrane proteins of primary and metastatic melanoma cells. *J Proteome Res* 2008;7: 1904–15.
31. Wallin E, von Heijne G. Genome-wide analysis of integral membrane proteins from eubacterial, archaean, and eukaryotic organisms. *Protein Sci* 1998;7:1029–38.
32. Fogel M, Gutwein P, Mechtersheimer S, et al. L1 expression as a predictor of progression and survival in patients with uterine and ovarian carcinomas. *Lancet* 2003;362:869–75.
33. Mamat S, Ikeda J, Enomoto T, et al. Prognostic significance of CUB domain containing protein expression in endometrioid adenocarcinoma. *Oncol Rep* 2010;23:1221–7.
34. Goto T, Kennel SJ, Abe M, et al. A novel membrane antigen selectively expressed on terminally differentiated human B cells. *Blood* 1994;84:1922–30.
35. Ohtomo T, Sugamata Y, Ozaki Y, et al. Molecular cloning and characterization of a surface antigen preferentially overexpressed on multiple myeloma cells. *Biochem Biophys Res Commun* 1999;258:583–91.
36. Walter-Yohrling J, Cao X, Callahan M, et al. Identification of genes expressed in malignant cells that promote invasion. *Cancer Res* 2003;63: 8939–47.
37. Kawai S, Azuma Y, Fujii E, et al. Interferon-alpha enhances CD317 expression and the antitumor activity of anti-CD317 monoclonal antibody in renal cell carcinoma xenograft models. *Cancer Sci* 2008;99:2461–6.
38. Wang W, Nishioka Y, Ozaki S, et al. HM1.24 (CD317) is a novel target against lung cancer for immunotherapy using anti-HM1.24 antibody. *Cancer Immunol Immunother* 2009;58: 967–76.
39. Neil SJ, Zang T, Bieniasz PD. Tetherin inhibits retrovirus release and is antagonized by HIV-1 Vpu. *Nature* 2008;451:425–30.
40. Jouvenet N, Neil SJ, Zhadina M, et al. Broad-spectrum inhibition of retroviral and filoviral particle release by tetherin. *J Virol* 2009;83: 1837–44.
41. Adams GP, Weiner LM. Monoclonal antibody therapy of cancer. *Nat Biotechnol* 2005;23: 1147–57.
42. Imai K, Takaoka A. Comparing antibody and small-molecule therapies for cancer. *Nat Rev Cancer* 2006;6:714–27.
43. Matsuda A, Suzuki Y, Honda G, et al. Large-scale identification and characterization of human genes that activate NF-kappaB and MAPK signaling pathways. *Oncogene* 2003;22:3307–18.
44. Shultz LD, Schweitzer PA, Christianson SW, et al. Multiple defects in innate and adaptive immunologic function in NOD/LtSz-scid mice. *J Immunol* 1995;154:180–91.
45. Mulgrew K, Kinneer K, Yao XT, et al. Direct targeting of alphavbeta3 integrin on tumor cells with a monoclonal antibody, Abegrin. *Mol Cancer Ther* 2006;5:3122–9.
46. Erikson E, Adam T, Schmidt S, et al. In vivo expression profile of the antiviral restriction factor and tumor-targeting antigen CD317/BST-2/HM1.24/tetherin in humans. *Proc Natl Acad Sci USA* 2011;108:13688–93.
47. Powles R, Sirohi B, Morgan G, et al. A phase I study of the safety, tolerance, pharmokinetics, antigenicity and efficacy of a single intravenous dose of AHM followed by multiple doses of intravenous AHM in patients with multiple myeloma. *Blood* 2001;98:165A.
48. Tai Y-T, Anderson KC. Antibody-based therapies in multiple myeloma. *Bone Marrow Res* 2011; 2011:924058.

IJC
International Journal of Cancer

SOCS-1 gene delivery cooperates with cisplatin plus pemetrexed to exhibit preclinical antitumor activity against malignant pleural mesothelioma

Kota Iwahori[1,2], Satoshi Serada[1], Minoru Fujimoto[1], Barry Ripley[3], Shintaro Nomura[4], Hiroyuki Mizuguchi[5], Kazuki Shimada[1,2], Tsuyoshi Takahashi[6], Ichiro Kawase[7], Tadamitsu Kishimoto[3] and Tetsuji Naka[1]

[1] Laboratory for Immune Signal, National Institute of Biomedical Innovation, Osaka, Japan
[2] Department of Respiratory Medicine, Allergy, and Rheumatic Diseases, Osaka University Graduate School of Medicine, Osaka, Japan
[3] Laboratory of Immune Regulation, Osaka University Graduate School of Frontier Biosciences, Osaka, Japan
[4] Faculty of Animal Bioscience, Nagahama Institute of Bio-Science and Technology, Shiga, Japan
[5] Laboratory of Stem Cell Regulation, National Institute of Biomedical Innovation, Osaka, Japan
[6] Department of Surgery, Osaka University Graduate School of Medicine, Osaka, Japan
[7] Osaka Prefectural Medical Center for Respiratory and Allergic Diseases, Osaka, Japan

Malignant pleural mesothelioma (MPM) is an aggressive tumor with poor prognosis for which an effective therapy remains to be established. This study investigated the therapeutic potential of gene delivery using suppressor of cytokine signaling 1 (SOCS-1), an endogenous inhibitor of intracellular signaling pathways, for the treatment of MPM. We infected MPM cells (MESO-4, H28 and H226) with adenovirus-expressing SOCS-1 vector to examine the effect of SOCS-1 overexpression on MPM cells. We evaluated the antitumor effect of *SOCS-1* gene delivery combined with cisplatin plus pemetrexed by cell proliferation, apoptosis and invasion assay. We also investigated the regulation of NF-κB and STAT3 signaling related to apoptotic pathways. Furthermore, we evaluated the inhibition of tumor growth by *SOCS-1* gene delivery combined with cisplatin plus pemetrexed *in vivo*. *SOCS-1* gene delivery cooperated with cisplatin plus pemetrexed to inhibit cell proliferation, invasiveness and induction of apoptosis in MPM cells. SOCS-1 regulated NF-κB and STAT3 signaling to induce apoptosis in MESO-4 and H226 cells. Furthermore, *SOCS-1* gene delivery cooperated with cisplatin plus pemetrexed to regulate NF-κB signaling and significantly inhibit tumor growth of MPM *in vivo*. These results suggest that *SOCS-1* gene delivery has a potent antitumor effect against MPM and a potential for clinical use in combination with cisplatin plus pemetrexed.

Key words: malignant pleural mesothelioma, SOCS-1, gene therapy, NF-κB, STAT3

Abbreviations: 7-AAD: 7-amino-actinomycin D; DAPI: 4′,6-diamidino-2-phenylindole; MOI: multiplicity of infection; MPM: malignant pleural mesothelioma; MTS: 3-(4,5-dimethylthiazol-2-yl)-5-(3-carboxymethoxy-phenyl)-2-(4-sulfophenyl)-2*H*-tetrazolium; SOCS-1: suppressor of cytokine signaling 1; siRNA: small interfering RNA; STR: short tandem repeat; TUNEL: terminal deoxynucleotidyl transferase-mediated dUTP nick-end labeling

Additional Supporting Information may be found in the online version of this article.

Grant sponsors: Ministry of Education, Culture, Sports, Science and Technology, Japan; Ministry of Health, Labour and Welfare, Japan
DOI: 10.1002/ijc.27611
History: Received 2 Dec 2011; Accepted 16 Apr 2012; Online 24 Apr 2012

Correspondence to: Tetsuji Naka, Laboratory for Immune Signal, National Institute of Biomedical Innovation, 7-6-8 Saito-Asagi, Ibaraki, Osaka 567-0085, Japan, Tel.: +81-72-641-9843, Fax: +81-72-641-9837, E-mail: tnaka@nibio.go.jp

Malignant pleural mesothelioma (MPM) is an aggressive tumor arising from the mesothelial cells of serosal cavities. MPM may be asymptomatic at the early stage and is sometimes observed incidentally during routine chest radiography. Common symptoms include chest pain and dyspnea, which are caused by tumor invasion of the chest wall or pleural effusion and occur late during disease progression. Therefore, complete surgical resection is not applicable in the majority of patients at the time of diagnosis of this disease. Although chemotherapy with cisplatin plus pemetrexed improves survival time for patients with unresectable MPM, the overall median survival time is only 12 months.[1] Among molecular-targeted therapies, epidermal growth factor receptor (EGFR) inhibitors and angiogenesis inhibitors have been tested for MPM but without therapeutic benefit.[2] MPM is often associated with past exposure to asbestos, in which case there is a long latency period, often exceeding 20 years, between first exposure to asbestos and diagnosis of MPM.[3] The number of deaths from MPM is expected to increase in the next 20 years worldwide where heavy use of asbestos has occurred.[3–6] Thus, there is a growing need for the development of new therapies to treat this disease.

Inflammation is considered to play a critical role in the development and progression of various cancers, including

MPM.[7] Asbestos-induced chronic inflammation is implicated in the pathogenesis of MPM. Tumor development and progression induced by an inflammatory response are thought to be mediated by an interaction between proinflammatory cytokines and pathways including NF-κB and STAT3 that promote antiapoptotic signaling.[8] It was reported that asbestos caused an increase in the expression of NF-κB and proinflammatory cytokines such as TNF-α and interleukin (IL)-6.[9–11] The suppressor of cytokine signaling (SOCS) family proteins participate in the negative regulation of cytokine responses by terminating the activation of multiple signaling pathways.[12–14] Among these, SOCS-1 is known as the most potent negative regulator of proinflammatory signaling including NF-κB and STAT3 pathways. SOCS-1 was reported to ubiquitinate NF-κB p65, inducing subsequent degradation by proteasome.[15] On the other hand, SOCS-1 interacts with phosphorylated tyrosine residues on JAK kinases to interfere with the activation of STAT proteins.[16,17] Epigenetic silencing of SOCS-1 is detected in human cancers, such as hepatocellular carcinoma, gastric carcinoma, multiple myeloma and pancreatic ductal neoplasm, and is implicated in cancer development.[18–22] However, the role of SOCS-1 in MPM have not yet been investigated.

Because MPM locates within the thoracic cavity and rarely displays widespread metastasis, gene transfer to the thoracic cavity makes this tumor uniquely accessible, thus facilitating the direct administration of novel therapeutic agents and subsequent analysis of treatment effects. Clinical trials involving intrapleural administration of adenoviral vectors to patients with MPM have demonstrated that intrapleural gene therapy using adenoviral vectors is safe and well tolerated by patients with MPM.[23,24] In the current study, we demonstrate the silencing of SOCS-1 in MPM cell lines and the antitumor effect of *SOCS-1* gene delivery against MPM *in vitro* and *in vivo*. Current first-line chemotherapy of MPM is cisplatin plus pemetrexed. Pemetrexed has shown modest activity as single agent in patients with MPM, and treatment with pemetrexed plus cisplatin resulted in superior survival time compared to treatment with cisplatin alone in patients with MPM.[1] Therefore, we evaluated combined cisplatin plus pemetrexed, the first-line chemotherapy of this disease, with *SOCS-1* gene delivery in the treatment of MPM.

Material and Methods

Cell lines

Mesothelioma cell lines H28 and H226 were purchased from American Type Culture Collection (Manassas, VA). Mesothelioma cell line ACC-MESO-4 (MESO-4) cell lines were purchased from RIKEN BRC cell bank (Tsukuba, Japan). The identity of each cell line was confirmed by DNA fingerprinting *via* short tandem repeat (STR) profiling on June 30, 2011. The method used for testing was multiplexed PCR amplification of eight STR loci (TH01, D5S818, D13S317, D7S820, D16S539, CSF1PO, vWA and TPOX), and amelogenin was performed using the PowerPlexTM16 System (Promega, Madison, WI). PCR-amplified fragments were analyzed with an ABI PRISM 310 Genetic Analyzer (Applied Biosystems, Foster City, CA). Then the fragments were typed based on allelic ladders. All the cells were cultured in RPMI 1640 (Wako, Osaka, Japan) with 10% fetal calf serum (FCS; HyClone Laboratories, Logan, UT), 100 IU/ml penicillin and 100 μg/ml streptomycin (Nacalai Tesque, Kyoto, Japan) at 37°C under a humidified atmosphere of 5% CO_2.

Reagents

Recombinant human IFN-γ, TNF-α and IL-6 were purchased from PeproTech (Rocky Hill, NJ). Recombinant-soluble IL-6 receptor (sIL-6R) was obtained from Chugai Pharmaceutical (Tokyo, Japan). Cis-platinum(II) diammine dichloride (cisplatin) was purchased from Sigma (St. Louis, MO). Pemetrexed disodium was purchased from Toronto Research Chemicals (Ontario, Canada). Recombinant-active caspase-3 and the caspase-3 inhibitor z-DEVD-fmk were purchased from BD Pharmingen (San Diego, CA).

Real-time PCR analysis

After 12 hr of serum starvation, mesothelioma cell lines (MESO-4, H28 and H226) and human PBMC were treated with 10 ng/ml of recombinant human IFN-γ (PeproTech) for 15 min. Total RNA was prepared from cells using an RNeasy Mini Kit (Qiagen, Valencia, CA), and cDNAs were synthesized from 200 ng of each total RNA preparation using a Quantitect Reverse Transcription Kit (Qiagen), all according to the manufacturer's instructions. The forward and reverse primers were as follows: for human SOCS-1 forward primer, 5′-AGACCCCTTCTCACCTCTTG-3′ and reverse primer, 5′-GCACAGCAGAAAAATAAAGC-3′; for β-actin, 5′-GTGGGGCGCCCCAGGCACCA-3′ and 5′-CTCCTTAATGTCACGCACGATTTC-3′.[25] Primers and cDNA were added to SYBR green premix (Invitrogen, Carlsbad, CA), which contained all the reagents required for PCR. The PCR conditions of SOCS-1 consisted of one cycle at 95°C for 10 min followed by 40–50 cycles of 96°C for 10 sec, 68°C for 15 sec and 72°C for 15 sec; β-actin cycling conditions consisted of one cycle at 95°C for 10 min followed by 40–50 cycles of 96°C for 10 sec, 67°C for 30 sec and 72°C for 30 sec. PCR products were measured continuously using the My IQ™ Single-Color Real-Time Detection System (Bio-Rad Laboratories, Hercules, CA).

Preparation of adenoviruses

Replication-defective recombinant adenoviral vector expressing the mouse *SOCS-1* gene was provided by Dr. Hiroyuki Mizuguchi (Osaka University, Osaka, Japan), which was constructed by an improved *in vitro* ligation method, as described previously.[26,27] An adenoviral vector expressing the LacZ gene was constructed using similar methods. Expression of these genes was regulated by Cytomegalovirus promoter/enhancer and intron A. The viruses were amplified in 293

cells. Viruses were purified by $CsCl_2$ step-gradient ultracentrifugation followed by $CsCl_2$ linear gradient ultracentrifugation. The purified viruses were dialyzed against a solution containing 10 mM Tris-HCl (pH 7.5), 1 mM $MgCl_2$ and 10% glycerol and were stored at −80°C. Viral particle and biological titers were determined by a spectrophotometrical method[28] and by using QuickTiter (Adenovirus Titer Immunoassay Kit, Cell Biolabs, San Diego, CA), respectively. After 24-hr incubation of MPM cells in culture medium containing 10% FCS, adenoviral vectors were infected by distributing suspensions onto cells at a multiplicity of infection (MOI) of 10–160.

MTS assay

MPM cell lines were plated in 96-well plates at a density of 1 × 10^3 cells per well and incubated in RPMI 1640 medium containing 10% FCS. After 72-hr culture, cell proliferation was evaluated with the 3-(4,5-dimethylthiazol-2-yl)-5-(3-carboxymethoxyphenyl)-2-(4-sulfophenyl)-2*H*-tetrazolium (MTS) assay (CellTiter 96 aqueous nonradioactive cell proliferation assay; Promega). MTS color development was measured and analyzed with a microplate reader Model 680 (Bio-Rad Laboratories) at a wavelength of 450 nm with a reference wavelength of 750 nm. This assay was performed in triplicate.

Apoptosis assay

MPM cells were grown to confluence to attain synchronization in G1 growth phase and subcultured at a lower density (1 × 10^5 cells in a six-well plate) for 24 hr so that most of the cells were in the S phase. Cells were infected with either adenoviral vector carrying SOCS-1 (AdSOCS-1) or AdLacZ as control at an MOI of 40. After 6 hr from infection, cells were cultivated with or without cisplatin (10 μM) plus pemetrexed (200 μM), followed by incubation at 37°C for an additional 72 hr. The cells were then trypsinized and collected with the supernatants, followed by determination of cell viability by means of annexin V and 7-amino-actinomycin D (7-AAD) staining (BD Biosciences, San Jose, CA) using the FACSCanto flow cytometer (BD Biosciences). Data were analyzed with FlowJo software (Tree Star, Ashland, OR). This assay was performed in triplicate.

Invasion assay

After 24-hr incubation of MPM cells in RPMI 1640 medium containing 10% FCS, adenoviral vectors were infected by distributing suspensions onto cells at an MOI of 40. Transfected cells were treated with cisplatin and pemetrexed in serum-free medium after 6 hr, and invasion assay was performed 24 hr after treatment using a Cultrex 96-well membrane invasion assay kit (R&D Systems, Minneapolis, MN) according to the manufacturer's instructions. Briefly, treated cells were harvested and seeded into the top chamber coated with 0.5 × BME at 5 × 10^4 cells per well. RPMI 1640 medium (150 μl) containing 10% FCS were added to each well of the bottom invasion chamber. The device was assembled and incubated at 37°C in an incubator containing 5% CO_2. After 36-hr incubation, the bottom plate was measured at 485 nm excitation and 520 nm emission. This assay was performed in triplicate.

SDS-PAGE and Western blot analysis

Whole-cell protein extract was prepared from MPM cells in RIPA buffer [10 mmol/l Tris-HCl (pH 7.5), 150 mmol/l NaCl, 1% (v/v) NP-40, 0.1% (w/v) SDS, 0.5% (w/v) sodium deoxycholate, 1 mmol/l Na_3VO_4 and 1× protease inhibitor cocktail (Roche Applied Science, Indianapolis, IN)]. Extracted proteins were resolved on SDS-PAGE and transferred to an Immobilon-P Transfer membrane (Millipore, Bedford, MA). The following antibodies were used: anti-phospho-NFκB p65, 1:1,000; anti-NFκB p65, 1:1000; anti-phospho-STAT3, 1:1,000; anti-survivin, 1:1,000; anti-XIAP, 1:1,000; anti-cleaved caspase-3, 1:500; anti-cleaved caspase-8, 1:500; anti-caspase-9, 1:500; anti-phospho-Akt (Ser473), 1:1,000; anti-Akt, 1:1,000 (all from Cell Signaling Technology, Danvers, MA), anti-STAT3, 1:1,000; anti-Lamin B, 1:500; anti-GAPDH, 1:1,000 (all from Santa Cruz Biotechnology, Santa Cruz, CA), anti-phospho-FAK (Tyr397), 1:1,000 (Biosource, Camarillo, CA), anti-FAK, 1:1,000 (BD Transduction Laboratories, San Jose, CA), anti-FLIP, 1:1,000 (Enzo life sciences, Plymouth Meeting, PA) and anti-SOCS1 antibody (1:500; IBL, Gunma, Japan), followed by a 1:5,000 dilution of donkey anti-rabbit or 1:5,000 dilution of sheep anti-mouse horseradish peroxidase-conjugated secondary antibodies (GE Healthcare Bio-Sciences, Piscataway, NJ) and visualized with Western Lightning ECL reagent (Perkin-Elmer, Boston, MA).

Nuclear and cytoplasmic extraction

Subcellular protein fractionation was performed using the Proteo JET™ cytoplasmic and nuclear protein extraction kit (Fermentas, Ontario, Canada) and by following the procedures as suggested by the manufacturer. Briefly, ten volumes of cell lysis buffer (with protease inhibitors) were added to one volume of packed cells. After vortexing for 10 sec and incubation on ice for 10 min, cytoplasmic proteins were separated from nuclei by centrifugation at 500 *g* for 7 min. Isolated nuclei were washed once with 500 μl of the nuclei washing buffer and then collected by centrifugation. The collected nuclear pellets were resuspended in ice-cold nuclear storage buffer, and volume of the nuclear lysis reagents was added to the mixtures to lysis the nuclei by shaking for 15 min at 4°C. Then nuclear lysate was collected after rinsing by centrifugation at 20,000 *g* for 12 min.

Small interfering RNA transfection

Commercial NF-κB p65 and STAT3 small interfering RNA (siRNA) were obtained from Qiagen. Cells were transfected with siRNA using Lipofectamine 2000 reagent (Invitrogen) according to the manufacturer's instructions. Nonspecific siRNA (Qiagen) was used as a negative control, and the

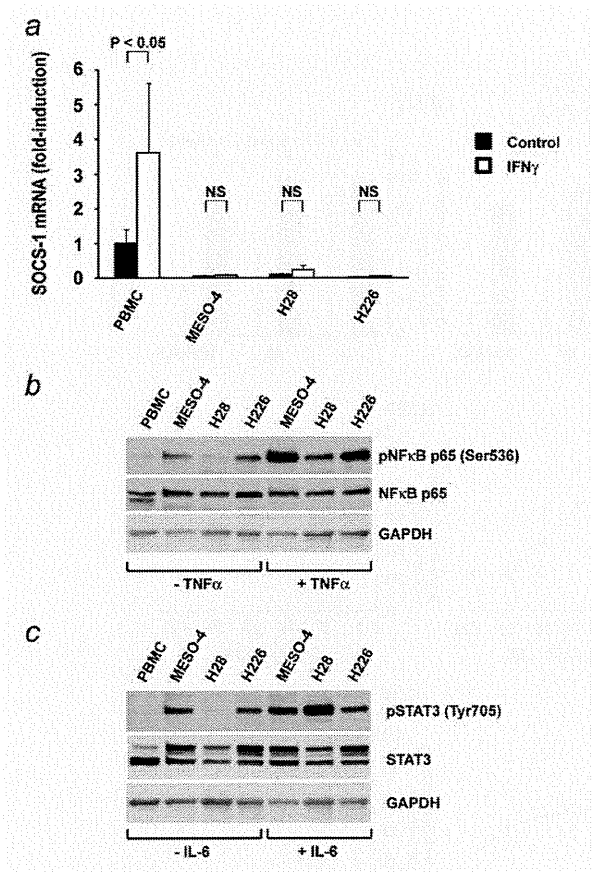

Figure 1. Expression of SOCS-1, NF-κB and STAT3 in MPM cell lines (MESO-4, H28 and H226). (*a*) Induction of the expression of *SOCS*-1 gene with or without stimulation with IFN-γ was analyzed by real-time PCR analysis. Values shown represent means + SD of triplicate measurements. NS means not significant. (*b*) Expression of endogenous NF-κB. After 12 h of serum starvation, MPM cells were treated with or without 10 ng/ml TNF-α for 30 min. Whole-cell extracts were analyzed by Western blotting. Human PBMC was prepared as a negative control. (*c*) Expression of endogenous STAT3. After 12 h of serum starvation, MPM cells were treated with or without 20 ng/ml IL-6 and sIL-6R for 15 min. Whole-cell extracts were analyzed by Western blotting. Human PBMC was prepared as a negative control.

selective silencing of p65 and STAT3 was confirmed by Western blot analysis.

DNA binding assay

NF-κB p65 and STAT3 activities were determined using TransAM Assay kit (Active Motif, Carlsbad, CA) according to the manufacturer's instructions. Briefly, nuclear extract was added to 96-well plates precoated with the oligonucleotide containing NF-κB p65 consensus sequence (5′-GGGACTTTCC-3′) or STAT3 consensus sequence (5′-TTCCCGGAA-3′), which is detected by sandwich ELISA. The absorbance was measured and analyzed with a microplate reader Model 680 (Bio-Rad Laboratories) at a wavelength of 450 nm. This assay was performed in triplicate.

Luciferase assay

MPM cell lines were plated in 24-well plates at a density of 3 × 10^4 cells per well. After 24-hr incubation of MPM cells in RPMI 1640 medium containing 10% FCS, adenoviral vectors were infected by distributing suspensions onto cells at an MOI of 40. The cells were harvested after 24 hr and were transfected with NF-κB p65 reporter (Stratagene, La Jolla, CA) or STAT3 reporter plasmid and pRL-TK plasmid (Promega) using Lipofectamine 2000 reagent (Invitrogen) according to the manufacturer's instructions. The STAT3 reporter containing the −478/−229 fragment of the *Stat3* promoter downstream of the minimal *junB* promoter luciferase gene (p478/229-Luc) was kindly provided by Dr. Toshio Hirano (Osaka University). Transiently transfected cells were treated with cisplatin and pemetrexed in serum-free medium after 6 hr, and luciferase activity was determined 24 hr after treatment using a dual-luciferase assay system (Promega) according to the manufacturer's instructions. Relative light units of Firefly luciferase activity were normalized with *Renilla* luciferase activity. This assay was performed in triplicate.

Mouse xenograft model

All animal experiments were conducted according to the institutional ethical guidelines for animal experimentation of the National Institute of Biomedical Innovation (Osaka, Japan). Female ICR *nu/nu* mice, 6–7 weeks of age, were obtained from Charles River Japan (Yokohama, Japan). The mice were housed for 7–14 days and allowed *ad libitum* access to food and water.

For pleural xenograft experiments, cells were resuspended in phosphate buffered saline (PBS) at a density of 1 × 10^6 cells in a total volume of 150 μl of 1/1 (v/v) PBS/Matrigel (Becton Dickinson). The mice were intrathoracically injected with 150 μl of the cell suspension through a 26-gauge needle. The mice were intrathoracically treated with 5 × 10^7 pfu/150 μl of AdSOCS-1 or AdLacZ on Days 10, 17 and 24 and intraperitoneally treated with pemetrexed (30 μg/g) on Days 10–14 and 17–21 along with cisplatin (2 μg/g) on Days 10 and 17 after the implantation of 1 × 10^6 MESO-4 or H226 cells into the pleural space. After 31 days of tumor cell inoculation, the mice were killed and their thoracic spaces examined macroscopically for growths, and tumors detected in the thoracic spaces were removed and weighed.

Immunohistochemistry

Tumors in the thoracic spaces were harvested and paraffin embedded for immunohistochemical analysis using anti-SOCS-1 antibody (Abcam, Cambridge, MA) and anti-NFκB p65 antibody (Santa Cruz Biotechnology). Terminal deoxynucleotidyl transferase-mediated dUTP nick-end labeling (TUNEL) assay [with 4′,6-diamidino-2-phenylindole (DAPI)

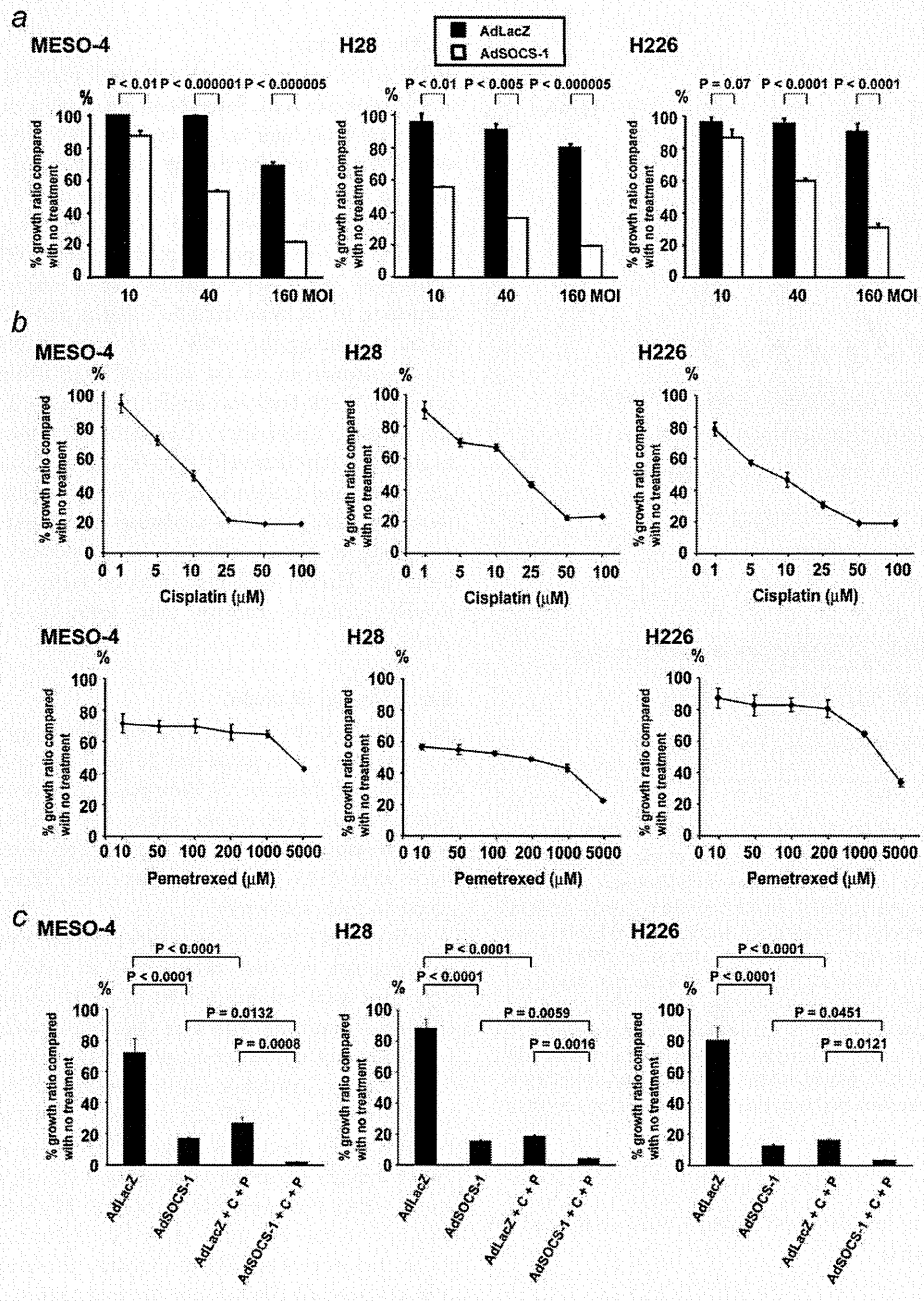

Figure 2. Effect of AdSOCS-1, cisplatin and pemetrexed on viability of MPM cell lines (MESO-4, H28 and H226). (a) Effect of AdSOCS-1 on viability of three MPM cell lines. Cells were infected with either AdSOCS-1 or AdLacZ. After a 72-hr culture, viable cell numbers were counted by MTS assay. Values shown represent means + SD of triplicate wells. (*b*) Effect of cisplatin and pemetrexed on viability of three MPM cell lines. Cells were cultivated in the presence of cisplatin (1–100 μM) or pemetrexed (10–5,000 μM). After 72 hr culture, cell viability was estimated using the MTS assay. Values shown represent means ± SD of triplicate wells. (*c*) Effect of combined AdSOCS-1 and cisplatin plus pemetrexed on viability of three MPM cell lines. Cells were infected with either AdSOCS-1 or AdLacZ as control at an MOI of 40. After 6 hr from infection, cells were cultivated with or without 10 μM cisplatin (C) plus 200 μM pemetrexed (P). After an additional 120-hr culture, cell viability was estimated using the MTS assay. Values shown represent means + SD of triplicate wells.

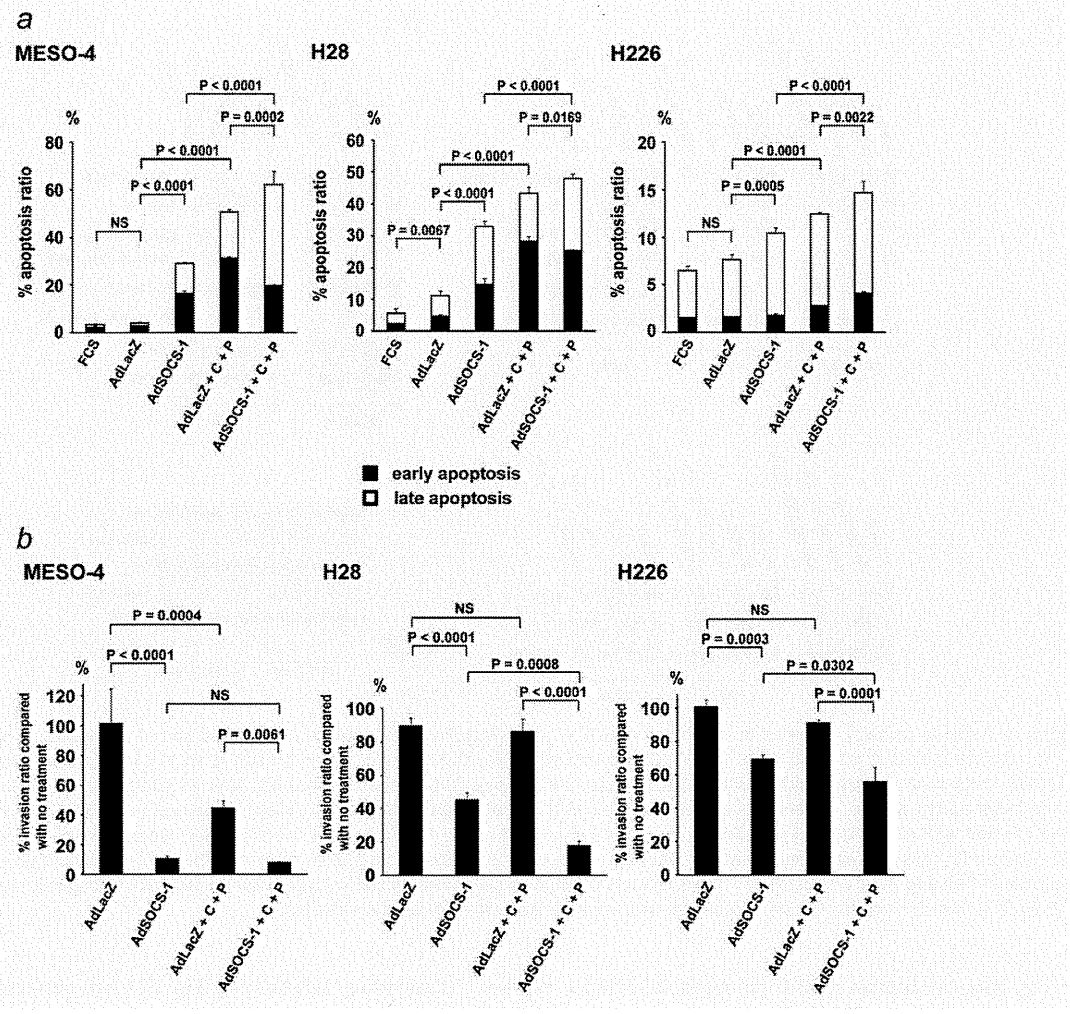

Figure 3. Apoptosis and cell invasion regulated by AdSOCS-1 combined with cisplatin and pemetrexed in MPM cell lines (MESO-4, H28 and H226). (*a*) Apoptosis assay. MPM cells were infected with either AdSOCS-1 or AdLacZ as control at an MOI of 40. After 6 hr from infection, cells were cultivated with or without 10 μM cisplatin (C) plus 200 μM pemetrexed (P). After an additional 72-hr culture, apoptosis was determined by means of annexin V and 7-AAD staining using flow cytometry. Values shown represent means + SD of triplicate wells. NS means not significant. (*b*) Cell invasion assay. MPM cells were infected with either AdSOCS-1 or AdLacZ as control at an MOI of 40. After 6 hr from infection, transfected cells were treated with or without 10 μM cisplatin (C) and 200 μM pemetrexed (P) in serum-free medium after 6 hr and invasion assay was performed 24 hr after treatment. Values shown represent means + SD of triplicate wells. NS means not significant.

nuclear counterstaining] for apoptosis was performed using the ApopTag® Fluorescein In Situ Apoptosis Detection Kit (Chemicon International, Temecula, CA) according to the manufacturer's instructions.

Statistical analysis

Data are shown as mean ± SD for the number of experiments indicated. To test for statistically significant differences between two groups, an unpaired Student's *t*-test was used. For comparisons among three or more groups, the values were analyzed by one-way ANOVA followed by Fisher's least significant difference *post hoc* comparisons. Differences were considered significant at $p < 0.05$.

Results

MPM cells fail to upregulate *SOCS-1* expression in response to IFN-γ

Reports of transcriptional silencing of *SOCS-1* in various types of cancer cells prompted us to investigate the levels of *SOCS-1* expression in MPM cells. By real-time PCR analysis, we found that three MPM cell lines (MESO-4, H28 and H226) did not upregulate *SOCS-1* expression in response to

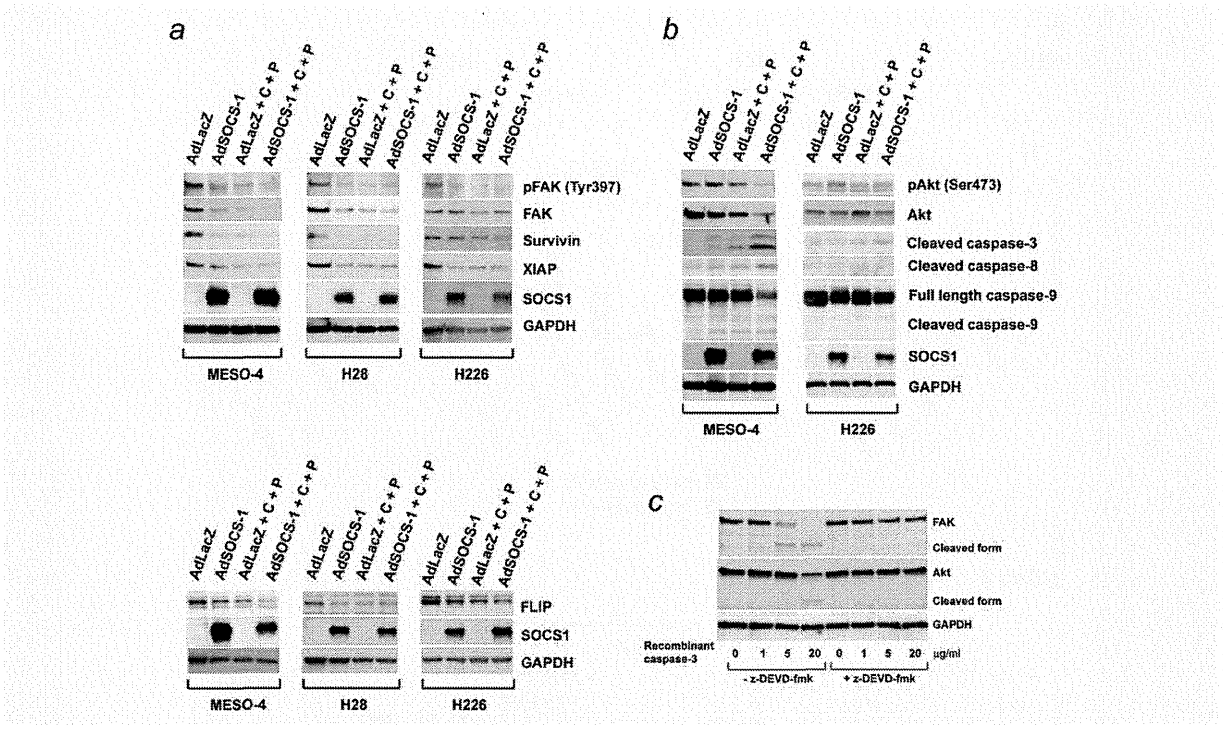

Figure 4. Caspase pathway activated by combined AdSOCS-1 and cisplatin plus pemetrexed. (*a*) Inhibition of antiapoptotic proteins. Three MPM cell lines (MESO-4, H28 and H226) were infected with either AdSOCS-1 or AdLacZ as control at an MOI of 40. After 6 hr from infection, cells were cultivated with or without 10 μM cisplatin (C) plus 200 μM pemetrexed (P). After an additional 24-hr (upper panel) or 48-hr (lower panel) culture, protein extracts were blotted with indicated antibodies. (*b*) Activation of caspases. MESO-4 and H226 cells were infected with either AdSOCS-1 or AdLacZ as control at an MOI of 40. After 6 hr from infection, cells were cultivated with or without 10 μM cisplatin (C) plus 200 μM pemetrexed (P). After an additional 72-hr culture, protein extracts were blotted with indicated antibodies. (*c*) Cleavage of FAK and Akt by caspase-3. Protein extracts of MESO-4 cells were incubated with recombinant active caspase-3 with or without z-DEVD-fmk. After 3 hr of incubation, protein extracts were blotted with indicated antibodies.

IFN-γ, whereas human PBMC upregulated *SOCS-1* expression in response to IFN-γ (Fig. 1*a*). Furthermore, *SOCS-1* transcript was underexpressed in three MPM cell lines (Fig. 1*a*). NF-κB and STAT3, which are known to be regulated by SOCS-1, were endogenously activated in MESO-4 and H226 cells (Figs. 1*b* and 1*c*). Under the condition stimulated by inflammatory cytokines TNF-α or IL-6, NF-κB and STAT3 were activated in all three MPM cell lines (Figs. 1*b* and 1*c*). Therefore, we subsequently delivered the *SOCS-1* gene to MPM cells to investigate the therapeutic efficacy of *SOCS-1* overexpression in MPM.

SOCS-1 gene delivery and cisplatin plus pemetrexed cooperate to exhibit antiproliferative effect in MPM cells

We used a replication-defective recombinant AdSOCS-1 to investigate the role of SOCS-1 in the regulation of MPM cell growth. AdSOCS-1 strongly inhibited cell growth of MESO-4, H28 and H226 cells in a dose-dependent manner (Fig. 2*a*). This indicates that overexpression of SOCS-1 was required for growth inhibition of MPM cells. Because sufficient transduction efficiency of the adenovirus vector and strong expression of SOCS-1 were detected at an MOI of 40 in MPM cells (Supporting Information Fig. S1), we performed subsequent experiments using AdSOCS-1 at an MOI of 40.

We next evaluated the therapeutic efficacy of cisplatin plus pemetrexed in the regulation of MPM cell growth. In three MPM cell lines, these compounds induced a dose-dependent decrease in cell viability with a cytotoxicity of >10 μM for cisplatin and 1 mM for pemetrexed (Fig. 2*b*). In view of evidence that AdSOCS-1 reduces cell viability, we sought to determine whether combination of pemetrexed, cisplatin and AdSOCS-1 would significantly reduce cell viability in MPM cells. To reveal a synergism between two chemotherapeutic molecules, each compound should be minimally toxic. Therefore, MOI 40 of AdSOCS-1 was combined to slightly cytotoxic doses of cisplatin (10 μM) and pemetrexed (200 μM). These concentrations are also within a dose range that can be achieved for chemotherapy of patients with MPM.

We therefore investigated the therapeutic efficacy of combined AdSOCS-1 and cisplatin plus pemetrexed under the concentrations described above. We found that AdSOCS-1 decreased cell growth inhibited by cisplatin plus pemetrexed ($p = 0.0008$, $p = 0.0016$ and $p = 0.0121$ for MESO-4, H28 and H226, respectively; Fig. 2*c*). Taken together, these

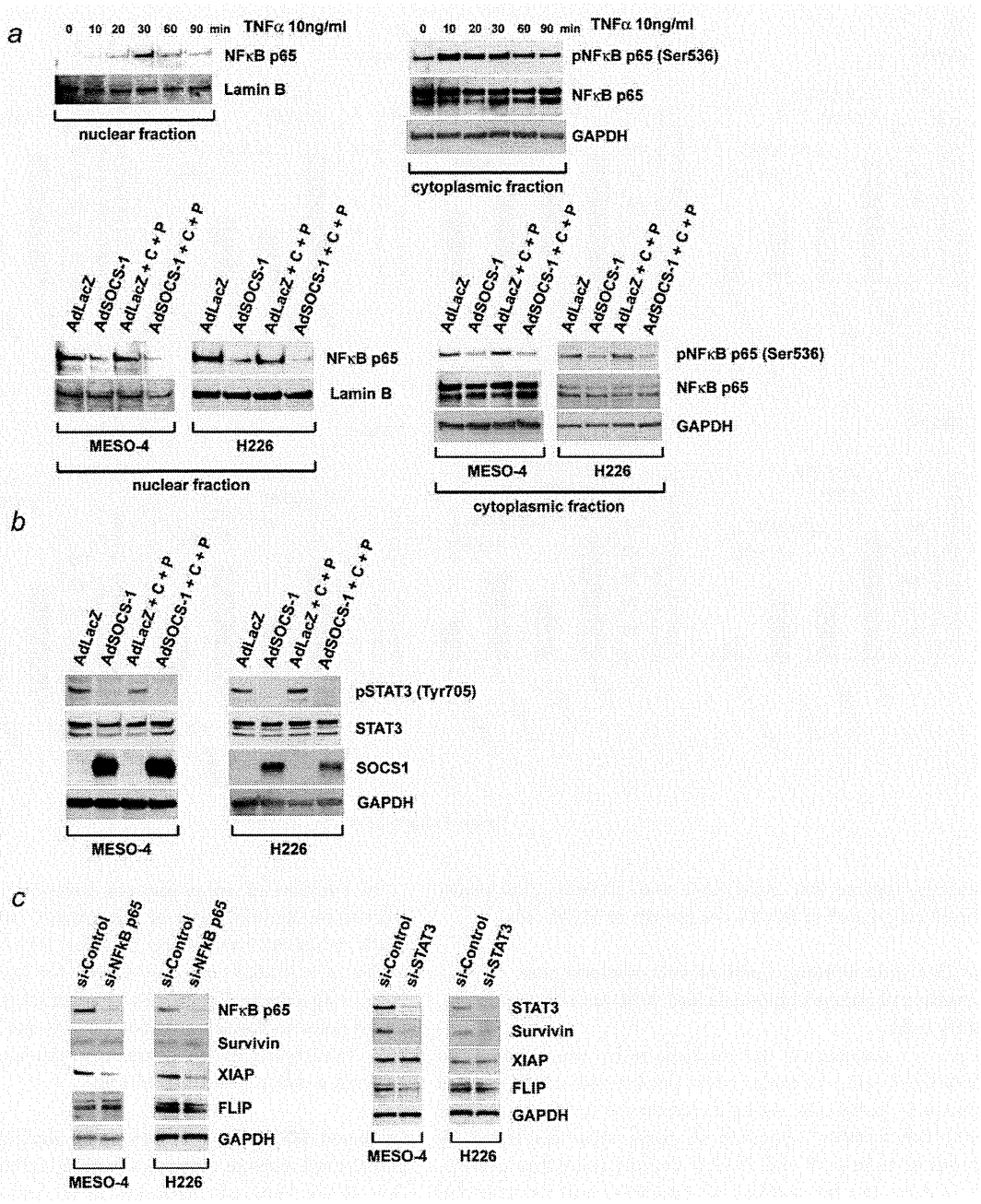

Figure 5. NF-κB and STAT3 signaling is regulated by AdSOCS-1. (*a*, upper panel) Activation of NF-κB p65 by TNF-α. After 12 hr of serum starvation, MESO-4 cells were incubated with 10 ng/ml TNF-α for 0–90 min. Cytoplasmic and nuclear fraction of protein extracts were blotted with indicated antibodies. (*a*, lower panel) Inhibition of NF-κB by SOCS-1. MESO-4 and H226 cells were infected with either AdSOCS-1 or AdLacZ as control at an MOI of 40. After 6 hr from infection, cells were cultivated with or without 10 μM cisplatin (C) plus 200 μM pemetrexed (P). After an additional 24-hr culture in serum-starved medium, MESO-4 and H226 cells were stimulated with 10 ng/ml TNF-α for 30 min. Cytoplasmic and nuclear fraction of protein extracts were blotted with indicated antibodies. (*b*) Inhibition of STAT3 by SOCS-1. MESO-4 and H226 cells were infected with either AdSOCS-1 or AdLacZ as control at an MOI of 40. After 6 hr from infection, cells were cultivated with or without 10 μM cisplatin (C) plus 200 μM pemetrexed (P). After an additional 24-hr culture, protein extracts were blotted with indicated antibodies. (*c*) Inhibition of antiapoptotic proteins by NF-κB p65 and STAT3. STAT3, NF-κB p65 or nonspecific siRNA as control was added to MESO-4 and H226 cells. After 24-hr culture, protein extracts were blotted with indicated antibodies. (*d*) DNA binding and luciferase assay of NF-κB p65 (upper panel) and STAT3 (lower panel). MESO-4 and H226 cells were infected with either AdSOCS-1 or AdLacZ as control at an MOI of 40. After 6 hr from infection, cells were cultivated with or without 10 μM cisplatin (C) plus 200 μM pemetrexed (P). After an additional 24-hr culture, cells were analyzed by DNA binding and luciferase assay. Values shown represent means + SD of triplicate wells. NS means not significant.

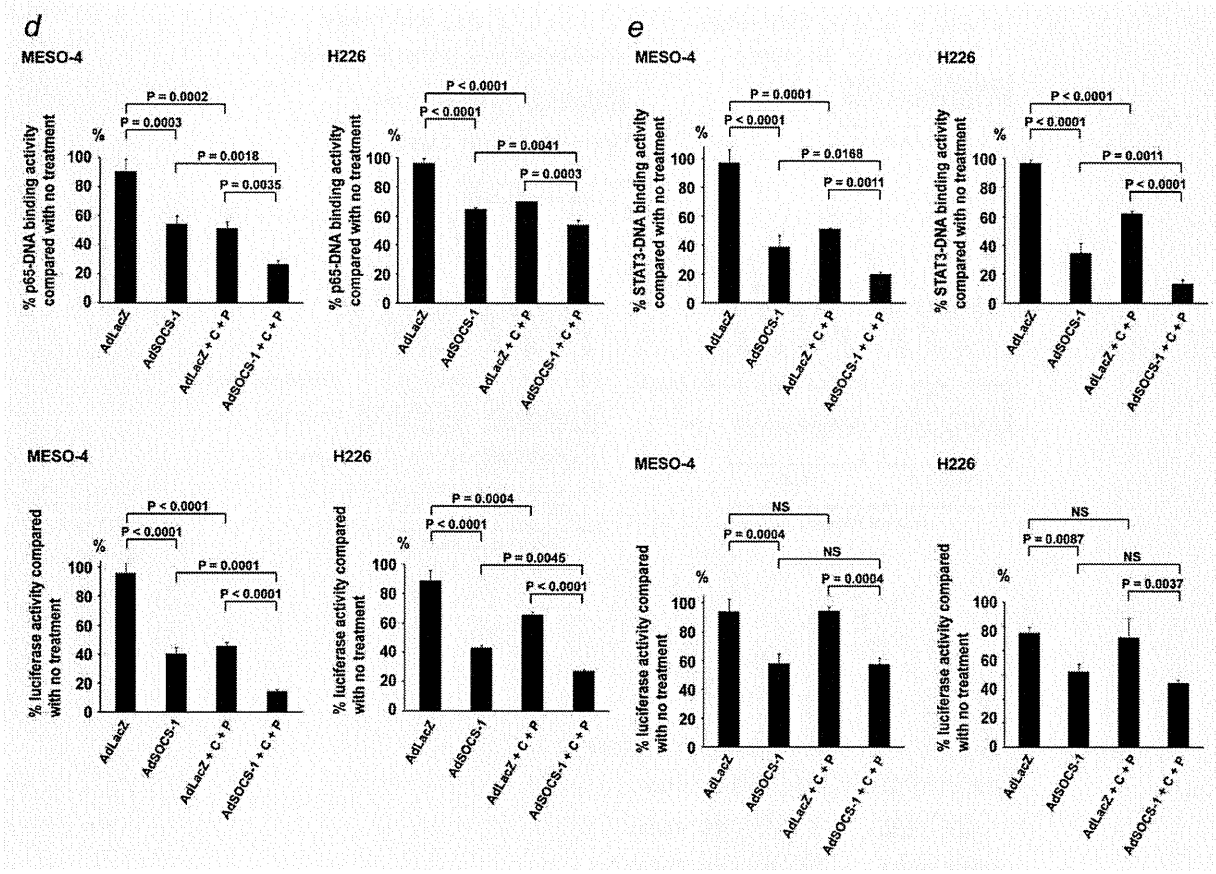

Figure 5. Continued

findings suggest that AdSOCS-1 and cisplatin plus pemetrexed cooperated to inhibit cell growth in MPM cells.

SOCS-1 gene delivery combined with cisplatin plus pemetrexed induced apoptosis and inhibited invasion in MPM cells

Next, we investigated the mechanism by which combined AdSOCS-1 and cisplatin plus pemetrexed inhibited cell growth in MPM cells. As light microscopy findings suggested poor cell viability, apoptosis in these cells was tested by means of annexin V and 7-AAD staining using flow cytometry 3 days after the addition of AdSOCS-1 and cisplatin plus pemetrexed to the culture. The results of flow cytometry analysis led to the identification of two types of cells: early apoptotic (AnnexinV$^+$7-AAD$^-$) and late apoptotic (Annexin V$^+$7-AAD$^+$). Compared to treatment with AdLacZ, treatment with AdSOCS-1 and cisplatin plus pemetrexed both resulted in elevated apoptosis in three MPM cell lines. Furthermore, AdSOCS-1 increased apoptosis induced by cisplatin plus pemetrexed ($p = 0.0002$, $p = 0.0169$ and $p = 0.0022$ for MESO-4, H28 and H226, respectively; Fig. 3*a*). These results suggest that AdSOCS-1 and cisplatin plus pemetrexed cooperated to induce apoptosis in MPM cells.

In addition to apoptosis, cell invasion is an important mechanism for inhibition of cell growth. AdSOCS-1 significantly inhibited invasiveness in three MPM cell lines ($p < 0.0001$, $p < 0.0001$ and $p = 0.0003$ for MESO-4, H28 and H226, respectively; Fig. 3*b*). By contrast, cisplatin plus pemetrexed failed to regulate invasion of H28 and H226 cells (Fig. 3*b*). Thus, regarding cell invasion, we estimate that AdSOCS-1 played a major role in MPM cells.

Combined *SOCS-1* gene delivery and cisplatin plus pemetrexed activate caspase signaling pathways

One of the important pathways in apoptosis is the caspase signaling pathway. Therefore, we investigated the regulation of caspases by AdSOCS-1 and cisplatin plus pemetrexed. We focused on antiapoptotic proteins survivin, FLIP and XIAP, which inhibit caspases.[29–31] Combined AdSOCS-1 and cisplatin plus pemetrexed inhibited survivin, FLIP and XIAP in MPM cells and activated caspases-3 and -9 in MESO-4 and H226 cells and caspase-8 in MESO-4 cells (Figs. 4*a* and 4*b*). Consistent with the cleavage of FAK and Akt by recombinant caspase-3, AdSOCS-1 and cisplatin plus pemetrexed inhibited FAK in MPM cells and Akt in MESO-4 cells, but AdSOCS-1 alone did not affect phospho-Akt in MESO-4 cells (Figs. 4*a*–

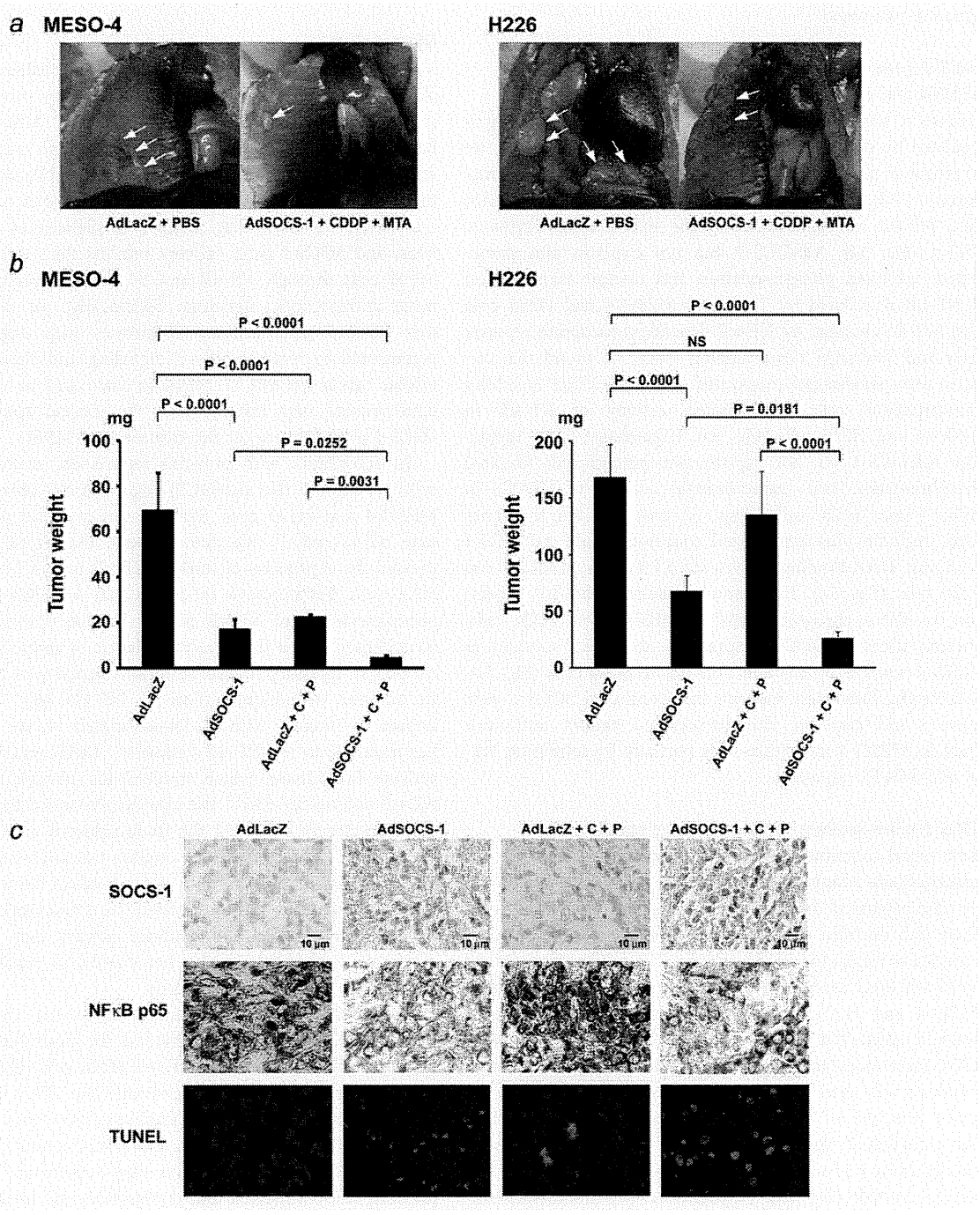

Figure 6. Antitumor effect of AdSOCS-1 combined with cisplatin and pemetrexed *in vivo*. (*a*) Gross appearance of MESO-4 and H226 tumors grown orthotopically in the thoracic spaces. Female ICR *nu/nu* mice were intrathoracically treated with AdSOCS-1 or AdLacZ and intraperitoneally treated with pemetrexed and cisplatin after the implantation of MESO-4 or H226 cells into the pleural space. (*b*) Each tumor nodule found in the thoracic spaces was also weighed. Values shown represent means + SD of five (MESO-4) or six (H226) mice. NS means not significant. (*c*) Immunohistochemical analysis of SOCS-1, NFκB p65 and TUNEL (blue fluorescence = DAPI staining for nuclei; cyan fluorescence = TUNEL positivity) in H226 tissue. The mice were treated in the same way as described above.